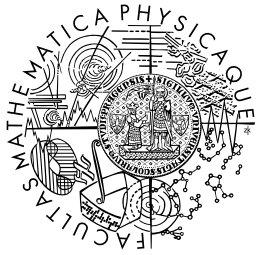

FACULTY
OF MATHEMATICS
AND PHYSICS
Charles University

BACHELOR THESIS

Martin Jurček

Spectrum of an operator characterizing the stability of the pipe flow

Mathematical Institute, Charles University

Supervisor of the bachelor thesis: Mgr. Vít Průša, Ph.D.
Study programme: Physics
Study branch: General Physics

Prague 2017

I declare that I carried out this bachelor thesis independently, and only with the cited sources, literature and other professional sources.

I understand that my work relates to the rights and obligations under the Act No. 121/2000 Sb., the Copyright Act, as amended, in particular the fact that the Charles University has the right to conclude a license agreement on the use of this work as a school work pursuant to Section 60 subsection 1 of the Copyright Act.

In ..... date ..... Martin Jurček

Title: Spectrum of an operator characterizing the stability of the pipe flow

Author: Martin Jurček

Institute: Mathematical Institute, Charles University

Supervisor: Mgr. Vít Průša, Ph.D., Mathematical Institute

Abstract: Stability is a fundamental property of a solution of a system of differential equations. If the system is represented by a linear differential operator, then the negativity of its spectrum implies the stability of the solution, where the negativity of the spectrum means the absence of eigenvalues with positive real part. The analysis of the spectrum of the corresponding linear operator is used in the study of the stability of the pipe flow. Unlike in other systems, there are no analytic formulas for the eigenvalues of the linearized operator characterizing the stability of the pipe flow and the eigenvalues must be computed numerically. Numerous numerical experiments indicate that the spectrum of the operator is negative, and the pipe flow is stable for all values of the Reynolds number. However, no formal proof of this statement exists so far. The objective of the thesis is to compare the spectrum of the operator characterizing the stability of the pipe flow with the spectrum of a simpler operator for which the analytic formulas for the eigenvalues are available. The comparison of the spectra of the operators might be helpful in formulating conjectures concerning the analytical estimates for the operator characterizing the stability of the pipe flow.

Keywords: flow stability, spectrum of differential operator, numerical solution

Název práce: Spektrum operátoru charakterizujícího stabilitu proudění v trubici

Autor: Martin Jurček

Ústav: Matematický ústav, Univerzity Karlovy

Vedoucí bakalářské práce: Mgr. Vít Průša, Ph.D., Matematický ústav

Abstrakt: Jednou ze základních vlastností řešení soustavy diferenciálních rovnic je stabilita. Pokud je soustava reprezentovaná lineárním diferenciálním operátorem, pak negativita příslušného spektra (absence vlastních čísel s kladnou reálnou částí) implikuje stabilitu daného řešení. Tato analýza spektra se využívá při studiu stability proudění ve válcové trubici. Pro vlastní čísla linearizovaného operátoru charakterizujícího stabilitu proudění v trubici ale neexistují analytické vztahy a vlastní čísla musí být počítána numericky. Numerické výpočty sice naznačují, že vlastní čísla jsou záporná a proudění v trubici je stabilní pro všechny hodnoty Reynoldsova čísla, formální důkaz tohoto tvrzení nám ale stále uniká. Cílem bakalářské práce je porovnat spektrum operátoru charakterizující stabilitu proudění v trubici se spektrem jednoduššího operátoru, pro jehož vlastní čísla máme analytické vztahy. Toto srovnání může být nápomocno při formulaci hypotézy pro analytický odhad spektra charakterizujícího proudění v trubici.

Klíčová slova: stabilita proudění, spektrum diferenciálního operátoru, numerické řešení

I would like to express my thanks to my supervisor, Mgr. Vít Průša, Ph.D. for all the academic guidance, patience and support. I am also grateful to my family and friends for all the kindness and support during the whole study.

Contents

Introduction

The basic and fundamental property of a solution of a system of differential equations is its stability under small perturbations of initial conditions. The stability determines the behavior of the solutions and indicates, for example, whether the given solution can be observed in experiment or not. If the system of differential equations is represented by a linear differential operator, then its spectrum characterizes the stability of the solution. This means that the whole stability problem reduces to the computation of the spectrum of the operator.

The question of the stability is very important while studying, for example, a flow of fluid. In 1883 Reynolds conducted a series of experiments in which he studied the stability of a flow in a pipe. He observed the transition from laminar to turbulent flow, and conjectured that the transition is related to the loss of stability of the laminar flow. This experiment encouraged many mathematicians to analyze this problem theoretically.

The stability of various flows was studied and various results were achieved. Plane Poiseuille flow, that is the motion of a fluid between two infinitely long parallel plates, has been studied, for example, in [1]. The numerical computations show the existence of a critical of value of the Reynolds number R_c

$$R_c = 5772.22,$$

for which the flow becomes unstable.

However, most of flows are less accessible to mathematical analysis in the sense that there are no analytic formulas or suitable estimates for the spectrum of the corresponding operator. This is especially true for the flow in a circular pipe (Hagen-Poiseuille flow, see: *Yudovich: Eleven great problems of mathematical hydrodynamics* [2]). The numerical results indicate that Hagen–Poiseuille pipe flow is *probably stable* for every value of the Reynolds number although no formal proof exists so far and the question of the stability of the Hagen–Poiseuille pipe flow remains unclear.

The subject of the thesis is to conduct numerical experiments and compute the eigenvalues of the operator that characterizes the stability of the pipe flow. Using the numerical results, we will show some basic properties of the spectrum of the operator characterizing the stability of the pipe flow (especially the absence of eigenvalues with positive real part). Further, we will compare the numerically found spectrum with the spectrum of a simpler, but similar operator for which analytic formulas for the eigenvalues are available. The simpler operator will be the Stokes operator. The comparison of the spectra might be helpful in formulating conjectures concerning the analytical estimates for the eigenvalues of the full operator characterizing the stability of the pipe flow.

The thesis is organized as follows. The asymptotic linear stability is defined in chapter 1. In chapter 2 we find the laminar solution for the Hagen–Poiseuille pipe flow. Further, we find the operator $\mathbb{L}$ that describes the stability of Hagen–Poiseuille pipe flow and introduce a similar, but simpler operator (Stokes operator $\mathbb{A}$) for which the analytic formulas for the eigenvalues are available. We summarize the derivation of these analytic formulas (see [3]). This analytic derivation seems to be an impossible task for the full operator $\mathbb{L}$.

In chapter 4 we describe the numerical methods used in the computation of the spectrum of the operator $\mathbb{L}$ (we use adopted Matlab algorithm, see Appendix A and [4]). In the last chapter we present the numerical results concerning the spectra of the operators. We discuss the convergence of the numerical approximation of the spectrum $\sigma(\mathbb{L})$ of the operator $\mathbb{L}$ and the spectrum of the Stokes operator $\sigma(\mathbb{A})$. Further, we plot the eigenvalues of the operator $\mathbb{L}$ with the largest real part $\max_{\lambda_i \in \sigma(\mathbb{L})} \Re(\lambda_i)$ as a function of the Reynolds number Re. This is the key piece of information from the perspective of the stability analysis. If $\max_{\lambda_i \in \sigma(\mathbb{L})} \Re(\lambda_i)$ is positive, then the flow is unstable, otherwise it is stable. We compare plots of $\max_{\lambda_i \in \sigma(\mathbb{L})} \Re(\lambda_i)$ as a function of Re for the full operator $\mathbb{L}$ and $\max_{\lambda_i \in \sigma(\mathbb{A})} \Re(\lambda_i)$ as a function of Re for the Stokes operator, and we comment on the behavior of these functions.

1. Asymptotic linear stability of the solution of differential equations

Let us consider a linear system of ordinary differential equations

$$\frac{\mathrm{d}x}{\mathrm{d}t} = \mathbb{A}x. \tag{1.1}$$

where $\mathbb{A}$ is a linear operator. In this section we will introduce a concept of the linear stability and asymptotic linear stability of the solution of (1.1) and formulate requirements that ensure the assymptotic linear stability. For more information see [5]

Definition 1. *The solution $x = \Phi(t)$ of (1.1) is stable if every solution $\psi(t)$ of (1.1) which starts sufficiently close to $\Phi(t)$ at $t = 0$ remains close to $\Phi(t)$ for all future time t. The solution $\Phi(t)$ is unstable if there exists at least one solution $\psi(t)$ of (1.1) which starts near $\Phi(t)$ at $t = 0$ but which does not remain close to $\Phi(t)$ for all future time. More precisely, the solution $\Phi(t)$ is stable if for every $\varepsilon > 0$ there exists $\delta = \delta(\varepsilon)$ such that*

$$||\psi(t) - \Phi(t)|| < \varepsilon \quad \textit{if} \quad ||\psi(0) - \Phi(0)|| < \delta(\varepsilon)$$

for every solution $\psi(t)$ of (1.1).

Definition 2. *A solution $x = \Phi(t)$ of (1.1) is asymptotically stable if it is stable, and if every solution $\psi(t)$ which starts sufficiently close to $\Phi(t)$ must approach $\Phi(t)$ as t approaches infinity.*

Theorem 1. *Every solution $x = \Phi(t)$ of (1.1) is asymptotically stable if all the eigenvalues of $\mathbb{A}$ have negative real part.*

Proof. Let $x = \Phi(t)$ be our solution of (1.1). We will first prove that if $x(t) \equiv 0$ is asymptotically stable, then $x = \Phi(t)$ is also asymptotically stable.

Let $\psi(t)$ by any solution of (1.1). Let us define $z(t) = \Phi(t) - \psi(t)$. It is evident that $z(t)$ is also a solution of (1.1). Therefore, if the solution $x(t) \equiv 0$ is stable, then $z(t) = \Phi(t) - \psi(t)$ will always remain small if $z(0) = \Phi(0) - \psi(0)$ is sufficiently small. Moreover, if $z(t)$ tends to 0 as t approaches infinity, then $\psi(t)$ approaches $\Phi(t)$ as t approaches infinity.

Now, let us prove that if all the eigenvalues if $\mathbb{A}$ have negative real part then $x(t) \equiv 0$ is asymptotically stable. Any solution of (1.1) is of the form: $\psi(t) = e^{\mathbb{A}t}\psi(0)$. Let us denote the ij element of the matrix $e^{\mathbb{A}t}$ as Ψ_{ij}. Then

$$\psi_i(t) = \sum_{j=1}^{n} \Psi_{ij}(t)\psi_j^0.$$

Let α_1 be the larges of the real parts of the eigenvalues. Each element of $\Psi_{ij}(t)$ is a linear combination of the of functions of the form $q(t)e^{\lambda t}$, where $q(t)$ is

a polynomial and λ is an eigenvalue. Then we can find a number K and α, $\alpha_1 < \alpha < 0$ such that

$$\left|\psi_i(t)\right| \leq \sum_{j=1}^{n} Ke^{\alpha t}\left|\psi_j^0\right| = Ke^{\alpha t}\sum_{j=1}^{n}\left|\psi_j^0\right|.$$

Hence

$$\|\psi(t)\| = max\{\left|\psi(t)\right|, ..., \psi_n(t)\} \leq nKe^{\alpha t}\|\psi(0)\|.$$

□

In the following example we will study the spectrum of the Laplace operator. Later on we will study more complicated systems which contain Laplacian.

1.1 Example: Stability of the trivial solution of the heat equation

Let us consider the heat equation in $\Omega \times \mathbb{R}^+ = (0,a) \times (0,b) \times \mathbb{R}^+ \subset \mathbb{R}^2 \times \mathbb{R}^+$ with the Dirichlet boundary condition.

$$\begin{aligned} \frac{\partial \phi}{\partial t} &= \Delta\phi, \\ \phi(0,y) &= \phi(a,y) = 0 \quad \forall y \in (0,b), \\ \phi(x,0) &= \phi(x,b) = 0 \quad \forall x \in (0,a). \end{aligned} \tag{1.2}$$

We immediately see that $\phi \equiv 0$ satisfies (1.2).

Let us investigate the stability of the previous solution. Let us denote the trivial solution of (1.2) as $\widetilde{\phi}$, $\widetilde{\phi} \equiv 0$, and a perturbation of the solution as ϕ. The sum of these two functions satisfies:

$$\begin{aligned} \frac{\partial(\phi + \widetilde{\phi})}{\partial t} &= \Delta\phi, \\ (\phi + \widetilde{\phi})(0,y) &= (\phi + \widetilde{\phi})(a,y) = 0 \quad \forall y \in (0,b), \\ (\phi + \widetilde{\phi})(x,0) &= (\phi + \widetilde{\phi})(x,b) = 0 \quad \forall x \in (0,a). \end{aligned} \tag{1.3}$$

Since $\widetilde{\phi}$ satisfies (1.2), system (1.3) reduces to:

$$\begin{aligned} \frac{\partial \phi}{\partial t} &= \Delta\phi, \\ \phi(0,y) &= \phi(a,y) = 0 \quad \forall y \in (0,b), \\ \phi(x,0) &= \phi(x,b) = 0 \quad \forall x \in (0,a). \end{aligned} \tag{1.4}$$

The trivial solution $\widetilde{\phi}$ is asymptotically stable if ϕ vanishes as t tends to infinity. The problem reduces to finding the eigenvalues λ and the eigenfunctions ϕ_{mn} of the Laplace operator that satisfy the boundary conditions:

$$\begin{aligned} \Delta\phi_{mn} &= \lambda_{mn}\phi_{mn}, \\ \phi_{mn}(0,y) &= \phi_{mn}(a,y) = 0 \quad \forall y \in (0,b), \\ \phi_{mn}(x,0) &= \phi_{mn}(x,b) = 0 \quad \forall x \in (0,a). \end{aligned} \tag{1.5}$$

We can easily show by using Green's theorem that the eigenvalues are negative. We take the foregoing partial differential equation, multiply it by ϕ_{nm} and integrate it over the volume Ω. We get

$$\int_\Omega \Delta\phi_{mn}\phi_{mn}\ dV = \int_\Omega \lambda_{mn}\phi_{mn}\phi_{mn}\ dV.$$

By using Green's theorem we get:

$$\int_\Omega \Delta\phi_{mn}\phi_{mn}\ dV = \int_{\delta\Omega} \phi_{mn}\nabla\phi_{mn}\ dS - \int_\Omega \nabla\phi_{mn}\cdot\nabla\phi_{mn}\ dV.$$

The first term of the left-hand side of the previous equation vanishes due to the boundary condition. Thus

$$\lambda_{mn}\int_\Omega \phi_{mn}\phi_{mn}\ dV = -\int_\Omega \nabla\phi_{mn}\cdot\nabla\phi_{mn}\ dV.$$

We can see that λ_{mn} is negative.

The system (1.5) can be solved by separation of variables. The resulting eigenfunctions are equal to

$$\phi_{mn} = \sin\left(\frac{\pi}{a}mx\right)\sin\left(\frac{\pi}{b}ny\right) \quad \text{for } m,n\in\mathbb{N},$$

and the corresponding eigenvalues are

$$\lambda_{nm} = -\pi^2\left(\frac{m^2}{a^2}+\frac{n^2}{b^2}\right).$$

The general solution of (1.4) can be written as:

$$\phi(x,y,t) = \sum_{m,n=1}^{\infty} a_{mn}(t)\phi_{mn}(x,y),$$

where

$$\phi_{nm}(x,y) = \sin\left(\frac{\pi}{a}mx\right)\sin\left(\frac{\pi}{b}ny\right),$$

and

$$\frac{da_{mn}}{dt} = \lambda_{mn}a_{mn},$$
$$a_{mn}(t) = C_{mn}e^{\lambda_{nm}t},$$

where C_{mn} is a constant. The limit of ϕ as t approaches infinity is zero as we expected. This means that the trivial solution of the heat equation is stable.

2. Pipe flow

In this chapter we study a flow in a pipe. We formulate the Navier-Stokes equations and find the laminar solution. Further, we find evolution equations for a perturbed system.

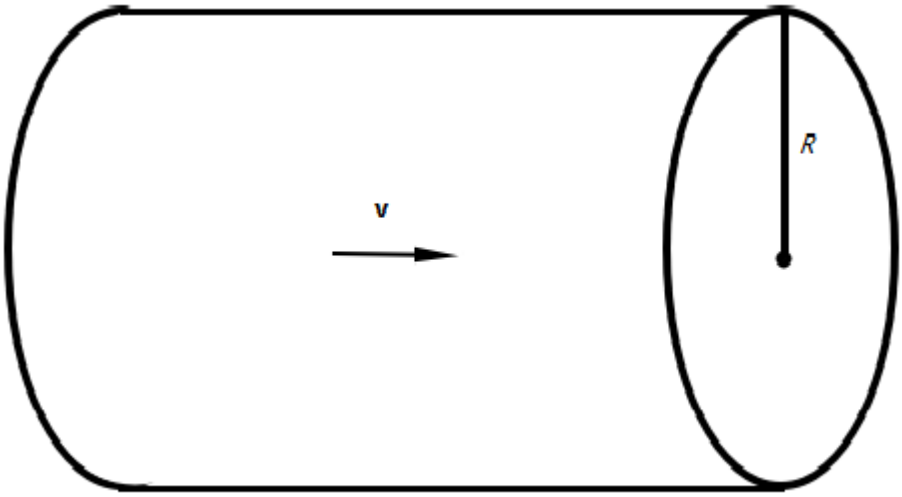

Figure 2.1: Pipe

2.1 Navier-Stokes equations and the laminar solution

Let us consider a flow in an infinite circular pipe of radius R, see figure 2.1, that is driven by the prescribed pressure gradient $\frac{\partial p}{\partial z}$. Furthermore, we consider a fluid to be incompressible and Newtonian. The density of the fluid is ρ and the dynamics viscosity is μ. The flow in the pipe is described by the system of partial differential equations known as the Navier-Stokes equations:

$$\begin{aligned} \nabla \cdot \boldsymbol{v} &= 0, \\ \rho \left[\frac{\partial \boldsymbol{v}}{\partial t} + (\boldsymbol{v} \cdot \nabla)\boldsymbol{v} \right] &= -\nabla p + \mu \Delta \boldsymbol{v}, \\ \boldsymbol{v}|_{\partial\Omega} &= 0, \end{aligned} \tag{2.1}$$

where $\partial\Omega = \{\boldsymbol{x} \in \mathbb{R}^3 : \boldsymbol{x} = (r, \varphi, z),\ r = R,\ \varphi \in (0, 2\pi),\ z \in (-\infty, \infty)\}$. The last equation represents the non-slip condition on the boundary.

Let us assume the flow to be steady and the velocity $\boldsymbol{v}$ depends only on the radial distance r, and pressure p depends only on position z. Therefore, in cylindrical coordinates we get

$$\frac{\partial \boldsymbol{v}}{\partial t} = 0,$$
$$u = 0, v = 0, w = w(r),$$

$$p = p(z),$$

where u, v, w are $x-$, $y-$, $z-$ component of $\boldsymbol{v}$, respectively. Then we can easily solve the system (2.1). Since

$$(\boldsymbol{v} \cdot \nabla)\boldsymbol{v} = 0,$$

and

$$\Delta \boldsymbol{v} = \frac{1}{r}\frac{\partial}{\partial r}\left(r\frac{\partial w}{\partial r}\right)\boldsymbol{e_z},$$

there is only one nontrivial equation:

$$\frac{1}{\mu}\frac{\partial p}{\partial z} = \frac{1}{r}\frac{\partial}{\partial r}\left(r\frac{\partial w}{\partial r}\right). \tag{2.2}$$

The solution of the preceding ordinary differential equation is:

$$w = \frac{1}{4\mu}\frac{\partial p}{\partial z}r^2 + C_1 \ln r + C_2. \tag{2.3}$$

where C_1 and C_2 are some constants. Considering the boundary condition (2.3), we obtain the final formula for the laminar solution of the flow in the pipe:

$$w = -\frac{1}{4\mu}\frac{\partial p}{\partial z}(R^2 - r^2). \tag{2.4}$$

2.2 Evolution equation for a perturbation

Let us consider the laminar flow with a small perturbation. The total velocity $\boldsymbol{v}_{tot}$ is equal to the sum of the velocity of laminar flow $\widetilde{\boldsymbol{v}}$ and the velocity of the perturbation $\boldsymbol{v}$:

$$\boldsymbol{v}_{tot} = \widetilde{\boldsymbol{v}} + \boldsymbol{v}.$$

We would like to study properties of the perturbation. At first we would like to find the evolution equations for the perturbation $\boldsymbol{v}$. We begin by formulating the Navier-Stokes equations for the full system:

$$\begin{aligned} \nabla \cdot (\widetilde{\boldsymbol{v}} + \boldsymbol{v}) &= 0, \\ \rho\left[\frac{\partial(\widetilde{\boldsymbol{v}} + \boldsymbol{v})}{\partial t} + ((\widetilde{\boldsymbol{v}} + \boldsymbol{v}) \cdot \nabla)(\widetilde{\boldsymbol{v}} + \boldsymbol{v})\right] &= -\nabla(\widetilde{p} + p) + \mu\Delta(\widetilde{\boldsymbol{v}} + \boldsymbol{v}), \\ (\widetilde{\boldsymbol{v}} + \boldsymbol{v})|_{\partial\Omega} &= 0. \end{aligned} \tag{2.5}$$

We already know that $\widetilde{\boldsymbol{v}}$ is the laminar solution of the Navier-Stokes equations. Subtracting (2.1) from (2.5), we get

$$\begin{aligned} \nabla \cdot \boldsymbol{v} &= 0, \\ \rho\left[\frac{\partial \boldsymbol{v}}{\partial t} + (\boldsymbol{v} \cdot \nabla)\widetilde{\boldsymbol{v}} + (\widetilde{\boldsymbol{v}} \cdot \nabla)\boldsymbol{v} + (\boldsymbol{v} \cdot \nabla)\boldsymbol{v}\right] &= -\nabla p + \mu\Delta\boldsymbol{v}, \\ \boldsymbol{v}|_{\partial\Omega} &= 0. \end{aligned} \tag{2.6}$$

If we consider the perturbation to be infinitesimal we can neglect the nonlinear term $(\boldsymbol{v} \cdot \nabla)\boldsymbol{v}$. Hence

$$\begin{aligned} \nabla \cdot \boldsymbol{v} &= 0, \\ \rho\left[\frac{\partial \boldsymbol{v}}{\partial t} + (\boldsymbol{v} \cdot \nabla)\widetilde{\boldsymbol{v}} + (\widetilde{\boldsymbol{v}} \cdot \nabla)\boldsymbol{v}\right] &= -\nabla p + \mu\Delta\boldsymbol{v}, \\ \boldsymbol{v}|_{\partial\Omega} &= 0. \end{aligned} \tag{2.7}$$

2.2.1 Evolution equation without convective terms

So far, we found the evolution equations for the perturbation. We can see that the convective terms $(\boldsymbol{v}\cdot\nabla)\widetilde{\boldsymbol{v}}$ and $(\widetilde{\boldsymbol{v}}\cdot\nabla)\boldsymbol{v}$ in (2.7) complicate the solution. Let us examine the behavior of the system if we omit these terms. Hence

$$\rho\frac{\partial \boldsymbol{v}}{\partial t} = -\nabla p + \mu\Delta\boldsymbol{v}. \tag{2.8}$$

Multiplying both sides of the foregoing equation by $\boldsymbol{v}$ and integrating over volume Ω we obtain

$$\int_\Omega \rho\frac{\partial \boldsymbol{v}}{\partial t}\cdot\boldsymbol{v}\,dV = -\int_\Omega \nabla p\cdot\boldsymbol{v}\,dV + \int_\Omega \mu\Delta\boldsymbol{v}\cdot\boldsymbol{v}\,dV. \tag{2.9}$$

The left-hand side of the foregoing equation can be written as the time derivative of the kinetic energy:

$$\int_\Omega \rho\frac{\partial \boldsymbol{v}}{\partial t}\cdot\boldsymbol{v}\,dV = \frac{d}{dt}\frac{1}{2}\rho\int_\Omega \boldsymbol{v}^2\,dV = \frac{dE}{dt}. \tag{2.10}$$

The first term of the right-hand side of (2.9) can be modified by using Green's theorem and obviously is equal to zero because of the zero-divergence condition and the boundary condition.

$$-\int_\Omega \nabla p\cdot\boldsymbol{v}\,dV = \int_\Omega p\,\nabla\cdot\boldsymbol{v}\,dV - \int_{\partial\Omega} p\,\boldsymbol{v}\cdot\boldsymbol{n}\,dS = 0 \tag{2.11}$$

The second term of right-hand side of the equation (2.9) can be written as

$$\int_\Omega \Delta\boldsymbol{v}\cdot\boldsymbol{v}\,dV = \int_{\partial\Omega}\nabla\boldsymbol{v}\,\boldsymbol{v}\cdot\boldsymbol{n}\,dS - \int_\Omega \nabla\boldsymbol{v}:\nabla\boldsymbol{v}\,dV = -\int_\Omega \nabla\boldsymbol{v}:\nabla\boldsymbol{v}\,dV, \tag{2.12}$$

where $\nabla\boldsymbol{v}:\nabla\boldsymbol{v}$ denotes $\mathrm{Tr}(\nabla\boldsymbol{v}\nabla\boldsymbol{v}^T)$. Thus from (2.9) we get

$$\frac{dE}{dt} = -\mu\int_\Omega \nabla\boldsymbol{v}:\nabla\boldsymbol{v}\,dV = -\mu\int_\Omega |\nabla\boldsymbol{v}|^2\,dV \le 0. \tag{2.13}$$

This means that if we omit the convective terms $(\boldsymbol{v}\cdot\nabla)\widetilde{\boldsymbol{v}} + (\widetilde{\boldsymbol{v}}\cdot\nabla)\boldsymbol{v}$ the perturbation will be subdued. This was a physical approach. Later we will proceed more mathematically. We will show that the eigenvalues of the Stokes operator $\mathbb{A}$, which characterize the system (2.8), are negative. This means that $\boldsymbol{v}$ tends to zero as t approaches infinity.

2.3 Non-dimensional Navier-Stokes and Stokes operator

Now we will non-dimensionalize the Navier-Stokes equations through choice of appropriate scales. The non-dimensional Navier-Stokes equations seems to be more convenient in our computation. We set

$$r^* = \frac{r}{L},\quad \boldsymbol{v}^* = \frac{\boldsymbol{v}}{V},\quad t^* = \frac{t}{L/V},\quad p^* = \frac{p}{\rho V^2},\quad Re = \frac{LV\rho}{\mu},$$

where L is the characteristic length (the radius of the pipe) and V is the characteristic velocity (velocity at the centreline). Using non-dimensional quantities (2.1) is of the form

$$\begin{aligned} \nabla \cdot \boldsymbol{v}^* &= 0, \\ \frac{\partial \boldsymbol{v}^*}{\partial t} + (\boldsymbol{v}^* \cdot \nabla)\boldsymbol{v}^* &= -\nabla p^* + \frac{1}{Re}\Delta \boldsymbol{v}^*, \\ \boldsymbol{v}^*|_{\partial\Omega} &= 0. \end{aligned} \tag{2.14}$$

From now on, we will work only with the non-dimensional Navier-Stokes equations and non-dimensional variables. For simplicity of notation we will denote the non-dimensional velocity, length, time and pressure as v, r, t and p respectively.

Let us return to the evolution equations for the perturbation. After scaling they take the following form

$$\begin{aligned} \nabla \cdot \boldsymbol{v} &= 0, \\ \frac{\partial \boldsymbol{v}}{\partial t} &= -\nabla p + \frac{1}{Re}\Delta \boldsymbol{v} - (\boldsymbol{v} \cdot \nabla)\widetilde{\boldsymbol{v}} - (\widetilde{\boldsymbol{v}} \cdot \nabla)\boldsymbol{v}, \\ \boldsymbol{v}|_{\partial\Omega} &= 0. \end{aligned} \tag{2.15}$$

3. Spectrum of the Stokes operator

In this chapter we investigate the evolution equations for the perturbation without the convective terms $(\boldsymbol{v}\cdot\nabla)\widetilde{\boldsymbol{v}}$ and $(\widetilde{\boldsymbol{v}}\cdot\nabla)\boldsymbol{v}$. We study the corresponding eigenvalue problem and find the analytic formulas for the eigenvalues and eigenfunctions of the Stokes operator $\mathbb{A}$.

The corresponding eigenvalue problem is of the form:

$$\begin{aligned} \nabla\cdot\boldsymbol{v} &= 0, && (3.1)\\ \lambda\boldsymbol{v} &= -\nabla p + \frac{1}{Re}\Delta\boldsymbol{v}, && (3.2)\\ \boldsymbol{v}|_{\partial\Omega} &= 0, && (3.3) \end{aligned}$$

where λ is the eigenvalue and $\boldsymbol{v}$ and p are the corresponding eigenfunctions. Further, we prescribe periodic boundary condition in z direction.

$$\boldsymbol{v}(r,\varphi,z,t) = \boldsymbol{v}(r,\varphi,z+2l,t) \tag{3.4}$$

3.1 Properties of the spectrum

Firstly, we show that the eigenvalues are negative. We proceed as above. We take the equation (3.2) multiple it by $\boldsymbol{v}$ and integrate it over a volume Ω

$$\int_\Omega \lambda\boldsymbol{v}\cdot\boldsymbol{v}\ dV = -\int_\Omega \nabla p\cdot\boldsymbol{v}\ dV + \frac{1}{Re}\int_\Omega \Delta\boldsymbol{v}\cdot\boldsymbol{v}\ dV. \tag{3.5}$$

Hence

$$\lambda\int_\Omega |\boldsymbol{v}|^2\ dV = -\frac{1}{Re}\int_\Omega |\nabla\boldsymbol{v}|^2\, dV. \tag{3.6}$$

It follows that all the eigenvalues are real and negative.

The preceding eigenvalue problem can be expressed by the Stokes operator $\mathbb{A}$ see [6]. It can be shown that the Stokes operator is self-adjoint and that the inverse of the Stokes operator is a compact operator. For the proof see [6]. It follows that

- $0 < \lambda_1 \le \cdots \le \lambda_j$,
- $\lim_{j\to\infty}\lambda_j = \infty$,
- Corresponding eigenfunctions form an orthonormal basis.

3.2 Analytic formulas for the eigenvalues and eigenfunctions

Now we summarize the derivation of the analytic formulas for the eigenvalues of the operator $\mathbb{A}$, performed in [3].

Let us consider the cylindrical domain Ω defined by

$$\Omega = \{\boldsymbol{x} \in \mathbb{R}^3 : \boldsymbol{x} = (r, \varphi, z),\ r \in (0,1),\ \varphi \in (0, 2\pi),\ z \in (-l, l)\}, \tag{3.7}$$

with the boundary $\partial\Omega$ compounded of two domains $\partial\Omega = \partial\Omega_1 \cup \partial\Omega_2$ defined by

$$\partial\Omega_1 = \{\boldsymbol{x} \in \mathbb{R}^3 : \boldsymbol{x} = (r, \varphi, z),\ r \in (0,1),\ \varphi \in (0, 2\pi),\ z \in \{-l, l\}\}, \tag{3.8}$$

$$\partial\Omega_2 = \{\boldsymbol{x} \in \mathbb{R}^3 : \boldsymbol{x} = (r, \varphi, z),\ r = 1,\ \varphi \in (0, 2\pi),\ z \in (-l, l)\}. \tag{3.9}$$

Ω represents the pipe of the radius $R = 1$ and length $2l$. $\partial\Omega_1$ and $\partial\Omega_2$ represent the base area and the lateral area, respectively.

Let us summarize the equations that describe our eigenvalue problem

$$\nabla \cdot \boldsymbol{v} = 0, \tag{3.10}$$

$$\lambda \boldsymbol{v} = -\nabla p + \frac{1}{Re}\Delta \boldsymbol{v}, \tag{3.11}$$

$$\boldsymbol{v}|_{\partial\Omega} = 0. \tag{3.12}$$

where $\boldsymbol{v}$ and p are the unknown functions velocity and pressure, respectively, and λ is the eigenvalue corresponding to $\boldsymbol{v}$ and p. Let us define new variables as

$$\widetilde{\boldsymbol{v}} = -\frac{\boldsymbol{v}}{Re}, \quad \widetilde{p} = -p, \quad \widetilde{\lambda} = -Re\lambda. \tag{3.13}$$

Then our eigenvalue problem takes a simpler form.

$$\nabla \cdot \widetilde{\boldsymbol{v}} = 0, \tag{3.14}$$

$$\widetilde{\lambda}\widetilde{\boldsymbol{v}} = \nabla\widetilde{p} - \Delta\widetilde{\boldsymbol{v}}, \tag{3.15}$$

$$\widetilde{\boldsymbol{v}}|_{\partial\Omega} = 0. \tag{3.16}$$

If we apply the divergence operator on (3.15) we get:

$$\Delta\widetilde{p} = 0. \tag{3.17}$$

In cylindrical coordinates equations (3.14), (3.15) and (3.16) take the form:

$$\widetilde{u}_r + r^{-1}\widetilde{v}_\varphi + \widetilde{w}_z + r^{-1}\widetilde{u} = 0, \tag{3.18}$$

$$\Delta\widetilde{u} - \frac{2}{r^2}\widetilde{v}_\varphi - r^{-2}\widetilde{u} + \widetilde{\lambda}\widetilde{u} = \widetilde{p}_r, \tag{3.19}$$

$$\Delta\widetilde{v} + \frac{2}{r^2}\widetilde{u}_\varphi - r^{-2}\widetilde{v} + \widetilde{\lambda}\widetilde{v} = r^{-1}\widetilde{p}_\varphi, \tag{3.20}$$

$$\Delta\widetilde{w} + \widetilde{\lambda}\widetilde{w} = \widetilde{p}_z, \tag{3.21}$$

$$\Delta\widetilde{p} = 0, \tag{3.22}$$

where $\widetilde{u}$, $\widetilde{v}$ and $\widetilde{w}$ are $r-$, $\varphi-$ and $z-$ component of $\widetilde{\boldsymbol{v}}$, respectively. Because of the symmetries of our problem we can write the solution as a superposition of functions in the following form:

$$\widetilde{\boldsymbol{v}}_{kn} = \widetilde{\boldsymbol{v}}_{kn}(r)\exp(in\varphi + ikz), \tag{3.23}$$

$$\widetilde{p}_{kn} = \widetilde{p}_{kn}(r)\exp(in\varphi + ikz). \tag{3.24}$$

where $n \in \mathbb{Z}$, $k = \frac{\pi}{l}m$, $m \in \mathbb{Z}$.
Introducing (3.23) and (3.24) into the foregoing equations we get:

$$\widetilde{u}'_{kn}(r) + r^{-1}\widetilde{u}_{kn}(r) + ik\widetilde{w}_{kn} + inr^{-1}\widetilde{v}_{kn} = 0. \tag{3.25}$$

$$\widetilde{u}''_{kn}(r) + r^{-1}\widetilde{u}'_{kn}(r) + \left(\widetilde{\lambda} - k^2 - \frac{n^2+1}{r^2}\right)\widetilde{u}_{kn}(r) - \frac{2in}{r^2}\widetilde{v}_{kn}(r) = \widetilde{p}'_{kn}, \tag{3.26}$$

$$\widetilde{v}''_{kn}(r) + r^{-1}\widetilde{v}'_{kn}(r) + \left(\widetilde{\lambda} - k^2 - \frac{n^2+1}{r^2}\right)\widetilde{v}_{kn}(r) + \frac{2in}{r^2}\widetilde{u}_{kn}(r) = \frac{in}{r}\widetilde{p}_{kn}, \tag{3.27}$$

$$\widetilde{w}''_{kn}(r) + r^{-1}\widetilde{w}'_{kn}(r) + \left(\widetilde{\lambda} - k^2 - \frac{n^2}{r^2}\right)\widetilde{w}_{kn}(r) = ik\widetilde{p}_{kn}, \tag{3.28}$$

$$\widetilde{p}''_{kn}(r) + \frac{1}{r}\widetilde{p}'_{kn}(r) - \left(k^2 + \frac{n^2}{r^2}\right)\widetilde{p}_{kn}(r) = 0. \tag{3.29}$$

We will study the solution of this system for the different cases of n and k.

The first important and the simplest case is $n = k = 0$. Then the formula (3.29) reduces to a simple ordinary differential equation called the Euler equation

$$\widetilde{p}''_{00}(r) + \frac{1}{r}\widetilde{p}'_{00}(r) = 0, \tag{3.30}$$

with the general solution

$$\widetilde{p}_{00} = C_1 + C_2 \ln r \qquad C_1, C_2 \in \mathbb{R}. \tag{3.31}$$

We set $C_2 = 0$ due to the boundedness of $\widetilde{p}_{00}$. Equations (3.26) - (3.28) reduce to

$$\widetilde{u}''_{00}(r) + r^{-1}\widetilde{u}'_{00}(r) + \left(\widetilde{\lambda} - \frac{1}{r^2}\right)\widetilde{u}_{00}(r) = 0, \tag{3.32}$$

$$\widetilde{v}''_{00}(r) + r^{-1}\widetilde{v}'_{00}(r) + \left(\widetilde{\lambda} - \frac{1}{r^2}\right)\widetilde{v}_{00}(r) = 0, \tag{3.33}$$

$$\widetilde{w}''_{00}(r) + r^{-1}\widetilde{w}'_{00}(r) + \widetilde{\lambda}\widetilde{w}_{00}(r) = 0, \tag{3.34}$$

with a general solution

$$\widetilde{u}_{\lambda 00}(r) = a_r J_1(\sqrt{\widetilde{\lambda}}r) + b_r Y_1(\sqrt{\widetilde{\lambda}}r), \tag{3.35}$$

$$\widetilde{v}_{\lambda 00}(r) = a_\varphi J_1(\sqrt{\widetilde{\lambda}}r) + b_\varphi Y_1(\sqrt{\widetilde{\lambda}}r), \tag{3.36}$$

$$\widetilde{w}_{\lambda 00}(r) = a_z J_0(\sqrt{\widetilde{\lambda}}r) + b_z Y_0(\sqrt{\widetilde{\lambda}}r), \tag{3.37}$$

where J_n denotes the Bessel function of order n and Y_n denotes the Weber function of order n. The terms corresponding to Weber function vanish because of the required boundedness in $r = 0$. At this point we confront the problem of satisfying the boundary condition $\widetilde{\boldsymbol{v}} = 0$ for $r = 1$. We have two choices how to fulfill the boundary condition. In the first case we set $a_z \neq 0$ and $a_r = a_\varphi = 0$. The values

of $\widetilde{\lambda}$ are restricted and $\sqrt{\widetilde{\lambda}}$ runs through all roots of the Bessel function of the zero order J_0 and the corresponding eigenfunctions are equal to

$$\widetilde{\boldsymbol{v}}_{\lambda 00} = a_z \begin{pmatrix} 0 \\ 0 \\ J_0(\sqrt{\widetilde{\lambda}} r) \end{pmatrix},$$

In the second case we set $a_z = 0$ and $a_\varphi \neq 0$, $a_r \neq 0$ and $\sqrt{\widetilde{\lambda}}$ runs through all roots of the Bessel function of the first order J_1. Moreover $a_r = 0$ because of the zero-divergence condition (3.18). Hence the corresponding eigenfunctions are

$$\widetilde{\boldsymbol{v}}_{\lambda 00} = a_\varphi \begin{pmatrix} 0 \\ J_1(\sqrt{\widetilde{\lambda}} r) \\ 0 \end{pmatrix}.$$

Analogously, similar formulas are obtained for the other cases. In the following section we just summarize the results of the derivation. For more information see [3].

In the case $n \neq 0$, $k = 0$ $\sqrt{\widetilde{\lambda}}$ runs either through all roots of J_n and the corresponding eigenfunctions are

$$\widetilde{\boldsymbol{v}}_{\lambda 0 n} = a_z \exp(in\varphi) \begin{pmatrix} 0 \\ 0 \\ J_n(\sqrt{\widetilde{\lambda}} r) \end{pmatrix},$$

or through all roots of J_{n+1} if $n > 0$ and through J_{n-1} if $n < 0$. Corresponding eigenfunctions are equal to

$$\widetilde{\boldsymbol{v}}_{\lambda 0 n} = c_1 \exp(in\varphi) \begin{pmatrix} \frac{|n| r^{|n|-1}}{\widetilde{\lambda}} + \frac{|n| J_n(\sqrt{\widetilde{\lambda}} r)}{r \widetilde{\lambda} J_n(\sqrt{\widetilde{\lambda}})} \\ in \left(\frac{r^{|n|-1}}{\widetilde{\lambda}} - \frac{(J_{n-1}(\sqrt{\widetilde{\lambda}}) - J_{n+1}(\sqrt{\widetilde{\lambda}}))}{2|n| \sqrt{\widetilde{\lambda}} J_n(\sqrt{\widetilde{\lambda}})} \right) \\ 0 \end{pmatrix}.$$

In the case $k \neq 0$ and $n = 0$ $\sqrt{\widetilde{\lambda}}$ is either equal to all roots of J_1 with corresponding eigenfunctions

$$\widetilde{\boldsymbol{v}}_{\lambda k 0} = a_\varphi \exp(ikz) \begin{pmatrix} 0 \\ J_1(\sqrt{\widetilde{\lambda} - k^2} r) \\ 0 \end{pmatrix},$$

or equal to all roots of the following equation

$$I_0(|k|) J_2(\sqrt{\widetilde{\lambda} - k^2}) + I_2(|k|) J_0(\sqrt{\widetilde{\lambda} - k^2}) = 0, \tag{3.38}$$

with corresponding eigenfunctions

$$\widetilde{\boldsymbol{v}}_{\lambda k 0} = c_1 \frac{\exp(ikz)}{\widetilde{\lambda}} \begin{pmatrix} ik \left(I_0(|k| r) - \frac{I_0(|k|) J_0(\sqrt{\widetilde{\lambda} - k^2} r)}{J_0(\sqrt{\widetilde{\lambda} - k^2})} \right) \\ |k| \left(I_1(|k| r) - \frac{I_1(|k|) J_1(\sqrt{\widetilde{\lambda} - k^2} r)}{J_1(\sqrt{\widetilde{\lambda} - k^2})} \right) \\ 0 \end{pmatrix}.$$

In the most general case $n \neq 0$ and $k \neq 0$ the values of $\widetilde{\lambda}$ are equal to the roots of the following determinant:

$$\begin{vmatrix} \sqrt{\widetilde{\lambda}-k^2}J_n(\sqrt{\widetilde{\lambda}-k^2})r & 0 & 2|k|I_n(|k|) \\ -J_{n-1}(\sqrt{\widetilde{\lambda}-k^2}) & J_{n-1}(\sqrt{\widetilde{\lambda}-k^2}) & I_{n-1}(|k|) \\ 0 & J_{n+1}\sqrt{\widetilde{\lambda}-k^2}) & I_{n+1}(|k|) \end{vmatrix} = 0. \tag{3.39}$$

The corresponding eigefunctions are equal to

$$\widetilde{\boldsymbol{v}}_{\lambda kn} = \exp\big(i(kz+n\varphi)\big) \begin{pmatrix} \widetilde{u}_{\lambda kn} \\ \widetilde{v}_{\lambda kn} \\ \widetilde{w}_{\lambda kn} \end{pmatrix},$$

where

$$\widetilde{u}_{\lambda kn} = \frac{a_r}{r}J_n(\sqrt{\widetilde{\lambda}-k^2}r) + \frac{ika_z}{\widetilde{\lambda}-k^2}J_{n-1}(\sqrt{\widetilde{\lambda}-k^2}r) + \tag{3.40}$$
$$+\frac{c_1|k|}{2\widetilde{\lambda}}(I_{n-1}(|k|r) + I_{n+1}(|k|r)),$$
$$\widetilde{v}_{\lambda kn} = -\frac{ka_z}{\widetilde{\lambda}-k^2}J_{n-1}(\sqrt{\widetilde{\lambda}-k^2}r) + \frac{c_1 i|k|}{2\widetilde{\lambda}}(I_{n-1}(|k|r) - I_{n+1}(|k|r)) + \tag{3.41}$$
$$+\frac{a_r i(\widetilde{\lambda}-k^2)}{2n}(J_{n-1}(\sqrt{\widetilde{\lambda}-k^2}r) - J_{n+1}(\sqrt{\widetilde{\lambda}-k^2}r)),$$
$$\widetilde{w}_{\lambda kn} = a_z J_n(\sqrt{\widetilde{\lambda}-k^2}r) + \frac{c_1 ik}{\widetilde{\lambda}}I_n(|k|r). \tag{3.42}$$

Finally, the eigenvalues of the Stokes system are equal to

$$\lambda = -\frac{\widetilde{\lambda}}{Re}. \tag{3.43}$$

The asymptotic behavior is Re^{-1} and the eigenvalues λ are negative for all $Re > 0$.

4. Numerical computation of the spectrum of the full operator

The computation of the spectrum of the full system is based on the approximation of the eigenfunctions by functions from a finite space, and projecting over a suitable space of functions. At first, we introduce some numerical techniques, see [4].

4.1 Chebyshev polynomials

In our numerical computation we will utilize a special family of orthogonal polynomials called Chebyshev polynomials. We will use these polynomials in a construction of differentiation matrices, where we will use a grid made of so-called Chebyshev points. We will also take advantage of these points in Gauss-Lobatto integration formulas and finally we will use Chebyshev polynomials to construct a suitable finite basis for approximating the eigenfunctions of the operator that characterize the stability of the pipe flow.

There are various equivalent options how to define Chebyshev's polynomials. The first possibility is based on the following ordinary differential equation:

$$(1-x^2)y'' - xy' + n^2 y = 0, \tag{4.1}$$

where the Chebyshev polynomials of degree n, T_n, arise as the solution of (4.1) for $n \in \mathbb{N}_0$. The second explicit and very useful definition is

$$T_n = \cos(n \arccos x), \tag{4.2}$$

which holds for $|x| \leq 1$.

At this moment, the point to note is that Chebyshev polynomials have many useful properties. We will mention just those that will be used in our later numerical computation. One of the most important property is the orthogonality. We say that Chebyshev polynomials are orthogonal with respect to the weight function w

$$w = \frac{1}{\sqrt{1-x^2}} \tag{4.3}$$

More precisely for $m, n \in \mathbb{N}_0$, $m \neq n$

$$\int_{-1}^{1} T_m(x) T_n(x) \frac{dx}{\sqrt{1-x^2}} = 0. \tag{4.4}$$

Second useful property is a parity. In general, Chebyshev polynomials are either even or odd, depending on the degree n

$$T_n(-x) = (-1)^n T_n(x). \tag{4.5}$$

We introduce two crucial set of points. The first set consists of the roots of Chebyshev polynomials on $[-1, 1]$

$$\xi_k^{(n)} = -\cos\left(\frac{2k-1}{2n}\pi\right), \tag{4.6}$$

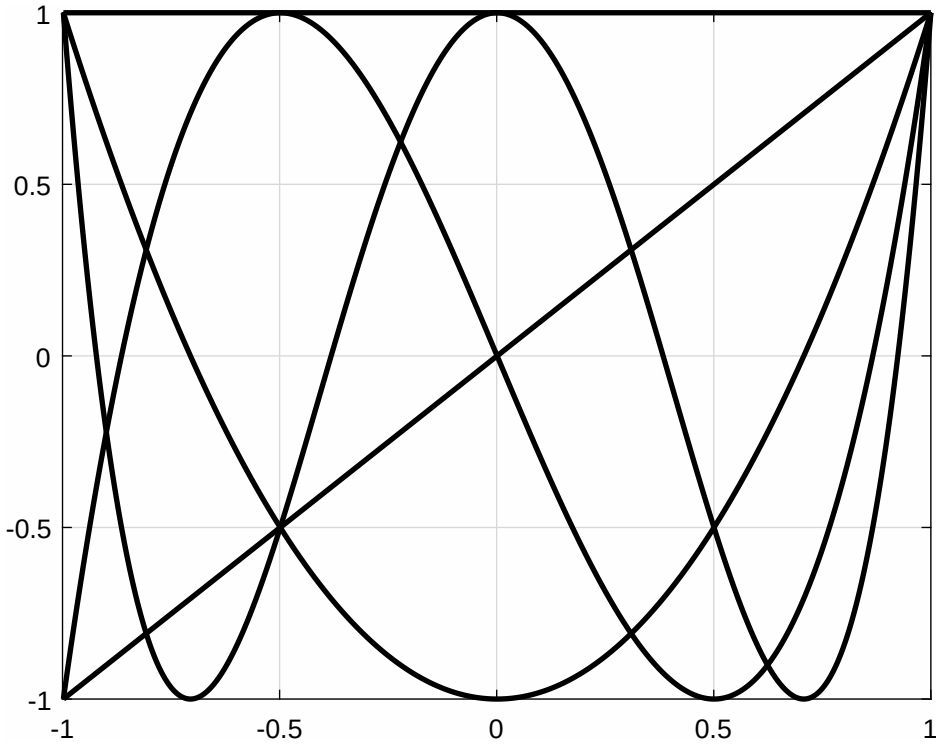

Figure 4.1: Chebyshev polynomials for $0 \leq n \leq 4$

where $1 \leq k \leq n$. The second set consists of the roots of the first derivative of Chebyshev polynomials and boundary points

$$\eta_k^{(n)} = -\cos\left(\frac{k\pi}{n}\right), \tag{4.7}$$

where $0 \leq k \leq n$. We will use these points in constructions of a grid for the differentiation matrices as well as in the Gauss-Lobatto integration formulas. More information about Chebyshev polynomials is discussed in [7] or [8].

4.2 Differentiation matrices

In many numerical computations we are facing the problem of computing an approximation of the first or higher derivative of a function f in fixed points $\{x_j\}_{j=1}^n$. One way how to accomplish this is an application of differentiation matrices. Let us suppose we know the values $f(x_j)$, $j = 1, ..., n$. There are various ways how to construct these matrices.

The first method is based on finite-differences. Let us have a uniform grid $\{x_j\}_{j=1}^n$. Then the first derivative of f in x_j can be approximated as followings

$$f'(x_j) \approx \frac{f(x_{j+1}) - f(x_{j-1})}{2h}. \tag{4.8}$$

Further let us assume that the problem is periodic with period n. This means

that $f(x_{n+1}) = f(x_1)$. This pattern leads to following differentiation matrix:

$$\begin{pmatrix} f'(x_1) \\ \vdots \\ f'(x_n) \end{pmatrix} \approx h^{-1} \begin{pmatrix} 0 & \frac{1}{2} & & & \frac{1}{2} \\ -\frac{1}{2} & 0 & \ddots & & \\ & & \ddots & & \\ & & \ddots & 0 & \frac{1}{2} \\ \frac{1}{2} & & & -\frac{1}{2} & 0 \end{pmatrix} \begin{pmatrix} f(x_1) \\ \vdots \\ f(x_n) \end{pmatrix}. \tag{4.9}$$

One can verify that the method will converge at the rate $O(h^2)$ for sufficiently smooth function f. Higher accuracy can be accomplished by using more terms of the Taylor expansions (4.8).

The second method is based on interpolating of f by a trigonometric or algebraic polynomial function. This might lead to spectral accuracy for analytic functions. It means that

$$\left|w_j - f'(x_j)\right| = O(h^m) \quad \forall m \geq 0.$$

where w_j is our approximation of the derivative of f in x_j.

Let us investigate the following situation. If we work on the interval $(-\infty, +\infty)$ or if we have periodic function f, then the approximation based on trigonometric polynomials and uniform grid of $\{x_j\}_{j=1}^n$ leads to spectral accuracy, provided f is smooth. Let us assume that we have a non-periodic function f defined on interval $[-1, 1]$. The question is how to choose the set of points $\{x_j\}$. It turns out that the uniform grid is not a good idea. This leads to Runge phenomenon and causes oscillations at the edges of the interval. This leads to a catastrophic loss of precision. It turns out that the density of the grid points should be asymptotically proportional to

$$\rho \sim \frac{n}{\pi\sqrt{1-x^2}}.$$

This dependence is more discussed in [9]. Chebyshev points $\{\eta_k^{(n)}\}_{k=0}^n$ defined as above satisfy the requirement and it is convenient to choose the set of points as: $\{x_j\} = \{\eta_k^{(n)}\}_{k=0}^n$. We can use these points to find interpolation polynomial φ of degree less or equal then n which satisfies $\varphi(x_j) = f(x_j) \quad \forall j = 0, ..., n$ and set $f'(x_j) \approx \varphi'(x_j) \quad \forall j = 0, ..., n$. It can be shown that if f is analytic in $[-1, 1]$ then this scheme leads to spectral precision. For the derivation of the corresponding differential matrix see [9]. Chebyshev differentiation matrix is equal to :

$$D_N = \begin{pmatrix} \frac{2n^2+1}{6} & 2\frac{(-1)^j}{1-x_j} & \cdots & 2\frac{(-1)^j}{1-x_j} & \frac{(-1)^n}{2} \\ -\frac{1}{2}\frac{(-1)^i}{1-x_i} & -\frac{x_j}{2(1-x_j^2)} & & \frac{(-1)^{i+j}}{x_i-x_j} & \frac{1}{2}\frac{(-1)^{n+i}}{1+x_i} \\ \vdots & & \ddots & & \vdots \\ -\frac{1}{2}\frac{(-1)^i}{1-x_i} & \frac{(-1)^{i+j}}{x_i-x_j} & & -\frac{x_j}{2(1-x_j^2)} & \frac{1}{2}\frac{(-1)^{n+i}}{1+x_i} \\ -\frac{(-1)^n}{2} & -\frac{2(-1)^{n+j}}{1+x_j} & \cdots & -\frac{2(-1)^{n+j}}{1+x_j} & -\frac{2n^2+1}{6} \end{pmatrix}.$$

The following code is an example of a function that takes the number of grid points and returns the Chebyshev differentiation matrix D_N. The same function for a construction of differentiation matrix is used in algorithm A (see Apendix - Matlab code rows 34-39).

```
1  function [D,x] = cheb(N)
2  if N==0, D=0; x=1; return, end
3  x = cos(pi*(0:N)/N)';
4  c = [2; ones(N-1,1); 2].*(-1).^(0:N)';
5  X = repmat(x,1,N+1);
6  dX = X-X';
7  D  = (c*(1./c)')./(dX+(eye(N+1)));
8  D  = D - diag(sum(D'));
```

4.2.1 Special form of differentiation matrices for boundary value problem and radial variable r

The differentiation matrix for the second derivative is equal to the square of D_N. In our numerical computation we will deal with a problem of computing the first and the second derivative of the function f satisfying the boundary condition $f(\pm 1) = 0$. Since the values of the function f at the boundary are $f(x_0) = f(x_n) = 0$, the first and the last column of D_n posses no relevant information. We can also ignore the values $f'(x_0)$ and $f'(x_n)$ since their values are no more relevant. Therefore, the differentiation matrix can be reduced by removing its first and last rows and columns.

In our computation we will work in cylindrical coordinates where $r \in [0, 1]$ instead of $[-1, 1]$. If take $r \in [-1, 1]$ instead of $r \in [0, 1]$ we can divide the differentiation matrix into four parts

$$D_N = \begin{pmatrix} D_{N1} & D_{N2} \\ D_{N3} & D_{N4} \end{pmatrix}. \tag{4.10}$$

The parts D_{N3} and D_{N4} can both be discarded because we don't need to know the values of $f'(r)$ for $r \leq 0$. In our following computation the functions we will differentiate will be either odd or even. For even functions the differentiation matrix is:

$$DE = D_{N1} + D_{N2} \tag{4.11}$$

for odd functions:

$$DO = D_{N1} - D_{N2} \tag{4.12}$$

For the computation of the odd and even differentiation matrices DE and DO see Appendix - Matlab code rows 43-48.

4.3 Numerical integration

In the computation of the spectrum of the operator characterizing the stability of the pipe flow we will have to integrate some functions. The only way how to accomplish this will be the application of numerical method.

Newton-Cotes quadrature formulas provide us the simplest tool how to numerically evaluate a general function. The idea is to take a uniform grid of points $\{x_i\}$, construct the Lagrange interpolant φ, where $f(x_i) = \varphi(x_i) \ \ \forall\ i = 0, \ldots, n$, and integrate φ analytically. In particular:

$$\begin{aligned}\int_a^b f(x)dx \approx \int_a^b \varphi(x)dx = \int_a^b \sum_{i=0}^{n} f(x_i) \prod_{j\neq i} \frac{x - x_j}{x_i - x_j} dx = \\ = \sum_{i=0}^{n} \int_a^b f(x_i) \prod_{j\neq i} \frac{x - x_j}{x_i - x_j} dx = \sum_{i=0}^{n} w_i f(x_i)\end{aligned} . \tag{4.13}$$

It can be shown that the formula

$$\int_a^b p(x)dx = \sum_{i=0}^{n} w_i p(x_i), \tag{4.14}$$

is true for any polynomial p of degree less or equal n. Thus, we say that the quadrature has order n.

Higher order can be obtained by using different grid of points $\{x_i\}$. The idea is to take the grid points obtained as a the roots of the first derivative of Chebyshev polynomials $\eta_k^{(n)}$ defined as above. This leads to Gauss-Lobatto integration formula:

$$\int_{-1}^{1} f(x)w\ dx \approx \sum_{i=0}^{n} f(\eta_i^{(n)})\widetilde{w}_i. \tag{4.15}$$

where $\widetilde{w}_i$ are weights of the quadrature and w is the weight function corresponding to the Chebyshev polynomials ($w = \frac{1}{\sqrt{1-x^2}}$). It can be shown that the Gauss-Lobbato integration quadrature (4.15) has order $2n - 1$. For more information see [7]. The weights $\widetilde{w}_i$ are equal to:

$$\widetilde{w}_i = \begin{cases} \frac{\pi}{2n} & \text{if} \quad i = 0 \quad \text{or} \quad i = n, \\ \frac{\pi}{n} & \text{if} \quad 1 \leq i \leq n-1. \end{cases} \tag{4.16}$$

For derivation see, for example, [7]. Later, we will deal with the fact of integrating f over the interval $(0, 1)$. This will be possible because of the evenness of the integrand.

$$\int_0^1 f(x)w\ dx = \frac{1}{2}\int_{-1}^{1} f(x)w\ dx. \tag{4.17}$$

If n is odd we can use only half elements in (4.15). In the algorithm the numerical integration is carried out by a matrix multiplication (see Appendix - Matlab algorithm rows 68-69).

4.4 The eigenvalue problem for the perturbation

The nondimensional Navier-Stokes equations for the perturbation are

$$\begin{aligned} \nabla \cdot \boldsymbol{v} &= 0, \\ \frac{\partial \boldsymbol{v}}{\partial t} &= -\nabla p + \frac{1}{Re}\Delta \boldsymbol{v} - (\boldsymbol{v} \cdot \nabla)\widetilde{\boldsymbol{v}} - (\widetilde{\boldsymbol{v}} \cdot \nabla)\boldsymbol{v}, \\ \boldsymbol{v}|_{\partial\Omega} &= 0, \end{aligned} \tag{4.18}$$

where $\boldsymbol{v}$ and p are non-dimensional velocity and pressure of the perturbation, $\widetilde{\boldsymbol{v}}$ is the velocity of the laminar flow and Re is the Reynolds number. Because of the symmetry of the problem we will work in cylindrical coordinates. Let us denote the r-, φ- and z- components of the velocity $\boldsymbol{v}$ (perturbation) as u, v, w, respectively, and the r-, φ- and z- components of the velocity $\widetilde{\boldsymbol{v}}$ (laminar solution) as $\widetilde{u}$, $\widetilde{v}$, $\widetilde{w}$, respectively.

In cylindrical coordinates (4.18) takes the form:

$$u_r + r^{-1}v_\varphi + w_z + r^{-1}u = 0, \tag{4.19}$$

$$u_t + \widetilde{w}u_z = -p_r + Re^{-1}(u_{rr} + r^{-1}u_r + r^{-2}u_{\varphi\varphi} + u_{zz} - 2r^{-2}v_\varphi - r^{-2}u), \tag{4.20}$$

$$v_t + \widetilde{w}v_z = -r^{-1}p_\varphi + Re^{-1}(v_{rr} + r^{-1}v_r + r^{-2}v_{\varphi\varphi} + v_{zz} + 2r^{-2}u_\varphi - r^{-2}v), \tag{4.21}$$

$$w_t + u\widetilde{w}_r + \widetilde{w}w_z = -p_z + Re^{-1}(w_{rr} + r^{-1}w_r + r^{-2}w_{\varphi\varphi} + w_{zz}). \tag{4.22}$$

The boundary condition takes the form:

$$u = v = w = 0 \quad for \quad r = 1. \tag{4.23}$$

Let the origin pressure be $\widetilde{p} = -4Re^{-1}z + K$, where K is a constant. Since $\widetilde{\boldsymbol{v}}$ is the laminar solution of the flow in a pipe we have $\widetilde{u} = 0$, $\widetilde{v} = 0$, $\widetilde{w} = -\widetilde{p}_z\frac{Re}{4}(1 - r^2) = 1 - r^2$. Due to periodicity we can write:

$$\boldsymbol{v}(r, \varphi, z, t) = e^{i(n\varphi+kz)}\boldsymbol{v}(r, t), \tag{4.24}$$

$$p(r, \varphi, z, t) = e^{i(n\varphi+kz)}p(r, t). \tag{4.25}$$

where $n \in \mathbb{Z}$, $k = \frac{\pi}{l}m$, $m \in \mathbb{Z}$. The resulting velocity and pressure are equal to the sum of the preceding functions over all n and k. Introducing (4.24) and (4.25) into the previous equations we get

$$u_t = -p_r + Re^{-1}(u_{rr} + r^{-1}u_r - r^{-2}n^2u - k^2u - 2r^{-2}inv - r^{-2}u) - ik\widetilde{w}u, \tag{4.26}$$

$$v_t = -inr^{-1}p + Re^{-1}(v_{rr} + r^{-1}v_r - r^{-2}n^2v - k^2v + 2r^{-2}inu - r^{-2}v) - ik\widetilde{w}v, \tag{4.27}$$

$$w_t = -ikp + Re^{-1}(w_{rr} + r^{-1}w_r - r^{-2}n^2w - k^2w) - \widetilde{w}_r u - ik\widetilde{w}w, \tag{4.28}$$

$$u_r + r^{-1}inv + ikw + r^{-1}u = 0. \tag{4.29}$$

Further, we can consider

$$\boldsymbol{v}(r, t) = \overline{\boldsymbol{v}}(t)\boldsymbol{v}(r). \tag{4.30}$$

$$p(r, t) = \overline{p}(t)p(r). \tag{4.31}$$

Our eigenvalue problem of the full system is of the form:

$$\begin{aligned} \nabla \cdot \boldsymbol{v} &= 0, \\ \lambda\boldsymbol{v} &= -\nabla p + \frac{1}{Re}\Delta\boldsymbol{v} - (\boldsymbol{v} \cdot \nabla)\widetilde{\boldsymbol{v}} - (\widetilde{\boldsymbol{v}} \cdot \nabla)\boldsymbol{v}, \\ \boldsymbol{v}|_{\partial\Omega} &= 0, \end{aligned} \tag{4.32}$$

where $\boldsymbol{v} = \boldsymbol{v}(r, \varphi, z)$, $p = p(r, \varphi, z)$ and λ is the eigenvalue corresponding to $\boldsymbol{v}$ and p. Proceeding as above we get:

$$-p_r + Re^{-1}(u_{rr} + r^{-1}u_r - r^{-2}n^2u - k^2u - 2r^{-2}inv - r^{-2}u) - ik\widetilde{w}u = \lambda u, \tag{4.33}$$

$$-inr^{-1}p + Re^{-1}(v_{rr} + r^{-1}v_r - r^{-2}n^2v - k^2v + 2r^{-2}inu - r^{-2}v) - ik\widetilde{w}v = \lambda v, \tag{4.34}$$

$$-ikp + Re^{-1}(w_{rr} + r^{-1}w_r - r^{-2}n^2w - k^2w) - \widetilde{w}_r u - ik\widetilde{w}w = \lambda w, \tag{4.35}$$

$$u_r - r^{-1}inv + ikw + r^{-1}u = 0 \tag{4.36}$$

where $\boldsymbol{v} = \boldsymbol{v}(r)$, $p = p(r)$. The foregoing eigenvalue problem (4.32) can be described by the linear operator $\mathbb{L}$. Then the system (4.32) reduces to

$$\mathbb{L}\boldsymbol{v} = \lambda\boldsymbol{v} \tag{4.37}$$

Later we will approximate $\boldsymbol{v}$ by a linear combination of functions from a space of functions that satisfy (4.36) identically.

But for the moment, let us investigate some numerical properties. In foregoing chapter dedicated to differential matrices we mentioned that we can achieve a spectral precision if the function we are working with is analytic. We will formulate a theorem that will ensure that the vector field $\boldsymbol{v}$ is analytic. For more information see [10].

Theorem 2. *Consider an analytic vector field* $\boldsymbol{v}(\varphi, r) = e^{in\varphi}\boldsymbol{v}(r) \quad n \in \mathbb{Z}$ *for* $r \leq \epsilon$ *for some* $\epsilon > 0$. *The radial, azimuthal and axial components of* $\boldsymbol{v}$ *must satisfy the following conditions:*

$$u = rf_E(r), \qquad v = rg_E(f) \quad if\ n = 0, \tag{4.38}$$

$$u = r^{|n|-1}f_E(r), \quad v = r^{|n|-1}g_E(f) \quad if\ n \neq 0, \tag{4.39}$$

for the radial and azimuthal components, and

$$w = r^{|n|}h_E(r) \quad \forall n \in \mathbb{Z}, \tag{4.40}$$

for the axial component, where f_E, g_E *and* h_E *are functions which are analytic and even.*

We can see that there is a requirement we will have to satisfy while constructing the suitable basis.

4.5 Petrov-Galerkin discretization

At this moment, our main goal is to find a suitable basis of functions that satisfy the zero-divergence condition, the boundary condition and theorem 2 to approximate our vector field $\boldsymbol{v}$. We seek the functions v_m such that:

$$v(r, \varphi, z) = e^{i(kz+n\varphi)} \sum_{m=0}^{2M} a_m v_m. \tag{4.41}$$

Since Chebyshev polynomials form an orthogonal basis we will use them in the construction of our basis. The zero-divergence condition makes the components of $\boldsymbol{v}$ linearly dependent and we have just two degrees of freedom for a particular $m = 0, 1..., M-1$. Let us define following two functions:

$$h_m(r) = (1-r^2)T_{2m}(r), \quad g_m(r) = (1-r^2)^2 T_{2m}(r), \tag{4.42}$$

where T_{2m} stands for the Chebyshev polynomial of degree $2m$. Let us investigate two cases depending on n.

In case that $n = 0$ (4.36) reduces to $u_r + ikw + r^{-1}u = 0$ so u and w are linearly dependent.

If $k \neq 0$ a suitable space of solenodial functions satisfying the boundary condition is composed of the following functions

$$v_m = \begin{pmatrix} 0 \\ rh_m(r) \\ 0 \end{pmatrix}, \; v_{m+M} = \begin{pmatrix} -ikrg_m(r) \\ 0 \\ (\frac{d}{dr} + r^{-1})[rg_m(r)] \end{pmatrix}.$$

For $k = 0$:

$$v_m = \begin{pmatrix} 0 \\ rh_m(r) \\ 0 \end{pmatrix}, \; v_{m+M} = \begin{pmatrix} -ikrg_m(r) \\ 0 \\ h_m(r) \end{pmatrix}.$$

The term r in the preceding functions is important to satisfy the parity requirements of theorem 2. The factor $(1-r^2)$ is added to satisfy the boundary condition.

In case $n \neq 0$ we proceed as above

$$v_m = \begin{pmatrix} -inr^{|n|-1}g_m(r) \\ \frac{d}{dr}[r^{|n|}g_m(r)] \\ 0 \end{pmatrix}, \; v_{m+M} = \begin{pmatrix} 0 \\ -ikr^{|n|+1}h_m(r) \\ inr^{|n|}h_m(r) \end{pmatrix}.$$

So far we have approximated $\boldsymbol{v}$ by the linear combination of the solenoidal functions v_m. Petrov-Galerkin method is based on approximating $\boldsymbol{v}$ by a linear combination of the functions from a finite dimensional space of solenoidal functions and projecting it over the function W from a suitable space. In particular, we are interested in a weak solution of our eigenvalue problem

$$(\mathbb{L}\boldsymbol{v}, W) = (\lambda \boldsymbol{v}, W), \tag{4.43}$$

where $(\cdot, \cdot)$ stands for the inner product. It is convenient to choose W as a function that satisfy the zero-divergence and the boundary condition. Then the pressure term in the operator $\mathbb{L}$ vanishes:

$$\int_\Omega \nabla p \cdot W \, dV = \int_{\partial\Omega} p \, W \cdot dS - \int_\Omega p \, \nabla \cdot W \, dV = 0. \tag{4.44}$$

Then the operator $\mathbb{L}$ takes the following form:

$$\mathbb{L}\boldsymbol{v} = \begin{pmatrix} Re^{-1}(u_{rr} + r^{-1}u_r - r^{-2}n^2u - k^2u - 2r^{-2}inv - r^{-2}u) - ik\widetilde{w}u \\ Re^{-1}(v_{rr} + r^{-1}v_r - r^{-2}n^2v - k^2v + 2r^{-2}inu - r^{-2}v) - ik\widetilde{w}v \\ Re^{-1}(w_{rr} + r^{-1}w_r - r^{-2}n^2w - k^2w) - \widetilde{w}_r u - ik\widetilde{w}w \end{pmatrix}. \tag{4.45}$$

We construct the functions W_m similar to the functions v_m but add the factor $\frac{1}{\sqrt{1-x^2}}$ which corresponds to Chebyshev weight. W is the linear combination of W_m.

Case $n = 0$, $k \neq 0$:

$$W_m = \frac{1}{\sqrt{1-r^2}} \begin{pmatrix} 0 \\ h_m(r) \\ 0 \end{pmatrix},$$

$$W_{m+M} = \frac{1}{\sqrt{1-r^2}} \begin{pmatrix} ikr^2 g_m(r) \\ 0 \\ (\frac{d}{dr} + r^{-1})[r^2 g_m(r)] + r^3 h_m(r) \end{pmatrix}.$$

Case $n = 0$, $k \neq 0$:

$$W_m = \frac{1}{\sqrt{1-r^2}} \begin{pmatrix} 0 \\ h_m(r) \\ 0 \end{pmatrix}, \; W_{m+M} = \frac{1}{\sqrt{1-r^2}} \begin{pmatrix} ikr^2 g_m(r) \\ 0 \\ r h_m(r) \end{pmatrix}.$$

Case $n \neq 0$

$$W_m = \frac{1}{\sqrt{1-r^2}} \begin{pmatrix} inr^s g_m(r) \\ \frac{d}{dr}[r^{1+s} g_m(r)] + r^{2+s} h_m(r) \\ 0 \end{pmatrix},$$

$$W_{m+M} = \frac{1}{\sqrt{1-r^2}} \begin{pmatrix} 0 \\ -ikr^{2+s} h_m(r) \\ inr^{1+s} h_m(r) r \end{pmatrix}$$

where $s = 1$ if n is odd otherwise $s = 0$. If $k = 0$ and n is odd, then the third component of W_{m+M} is replaced by $inh_m(r)$.

The computation of the basis $\{v_m\}$ and $\{W_m\}$ is carried out by functions V and W (see Appendix - Matlab code rows 70-102). The factor $\frac{1}{\sqrt{1-r^2}}$ is omitted because of the numerical quadrature. On the other hand, the factor $\frac{\pi}{N}$ is included because of the Gauss-Lobatto integration formula. Weights corresponding to $i = 0$ or $i = n$ are omitted due to the boundary condition.

Our eigenvalue problem (4.32)

$$\lambda \sum_{m=0}^{2M} a_m v_m = \sum_{m=0}^{2M} a_m \mathbb{L} v_m, \tag{4.46}$$

takes after projecting over the functions W_j the following form:

$$\lambda \mathbb{B} a = \mathbb{A} a, \tag{4.47}$$

where $\mathbb{B}_{ij} = (v_i, W_j)$ and $\mathbb{A}_{ij} = (\mathbb{L} v_i, W_j)$. Algorithm (Appendix A) returns matrices $\mathbb{A}$ and $\mathbb{B}$. The formula (4.47) is a generalized eigenvalue problem which can be solved by the built-in Matlab function *eig*.

5. Numerical results

In this section we present the numerical results. We begin by investigating the convergence of the method. The key piece of information is the negativity of the spectrum, where the negativity of the spectrum means the absence of eigenvalues with positive real part. We study the dependence of the eigenvalue with the largest real part $\max_{\lambda_i \in \sigma(\mathbb{L})} \Re(\lambda_i)$ on the Reynolds number for the operator $\mathbb{L}$ and the Stokes operator, and compare these results. See appendix A for the Matlab algorithm.

5.1 Convergence of the numerical method

At first we study the convergence of the numerical method. We investigate the dependence of $\max_{\lambda_i \in \sigma(\mathbb{L})} \Re(\lambda_i)$ on the number of Chebyshev modes for the radial approximation. In figure 5.1 we see this dependence for $k = n = 1$ and we can see that the algorithm convergences to a particular value.

We observe that there is a minimal value M_0 for Chebyshev modes to give correct results. Similar results are obtained for all cases $k \neq 0$. If $k = 0$ the method converges almost immediately. We see that the method converges but at the formal level we don't know if the value the method converges to is the right solution. We apply the numerical method for the computation of the eigenvalues

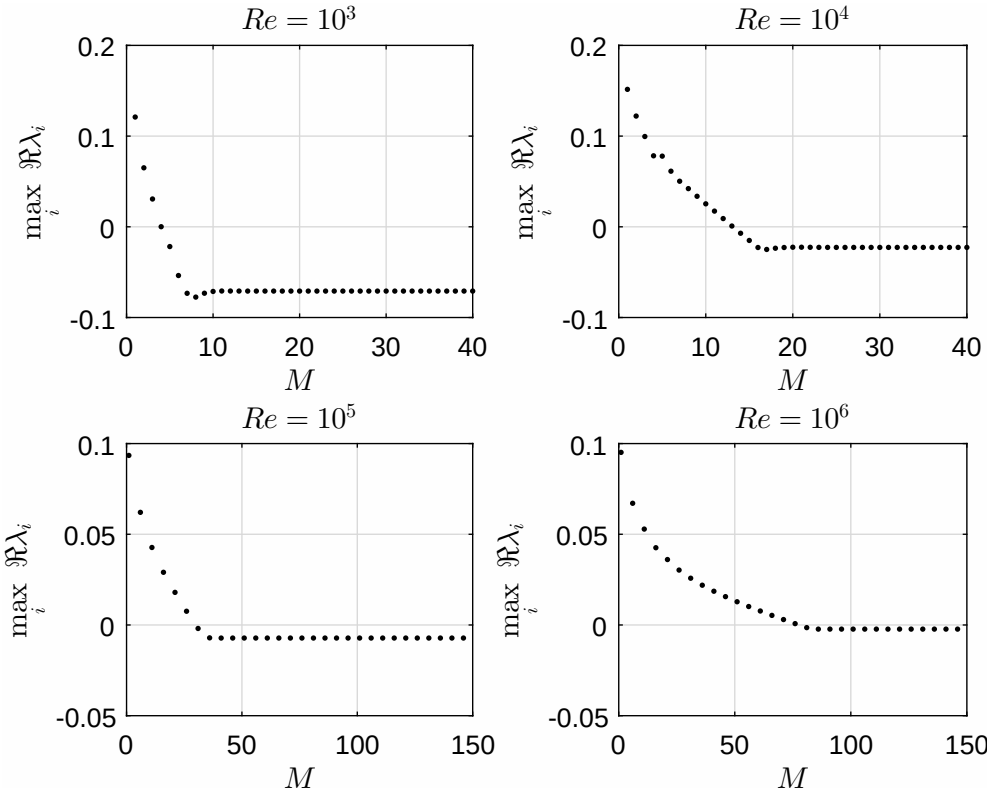

Figure 5.1: The dependence of the largest real part of the computed eigenvalues on the number of Chebyshev modes for radial approximation M

of the Stokes operator. Because we know the analytic formulas for the eigenvalues of the Stokes operator we can verify whether the algorithm converges to the right solution, at least for the case of the Stokes operator. The only thing we have to change in algorithm is to set $Lam = 0$ and $dLam = 0$ see Appendix A - Matlab code, row 61. In figure 5.2 we can see the dependence of the largest real part of the computed eigenvalues of the Stokes operator $\max_{\lambda_i \in \sigma(\mathbb{A})} \Re(\lambda_i)$ on the number of Chebyshev modes for radial approximation (represented by points). The dashed line shows the largest eigenvalue computed by analytic formula (3.39). In the case of the Stokes operator, we can see that the algorithm converges to the right value. This indicates that the algorithm should converge to the right solution for the full operator too.

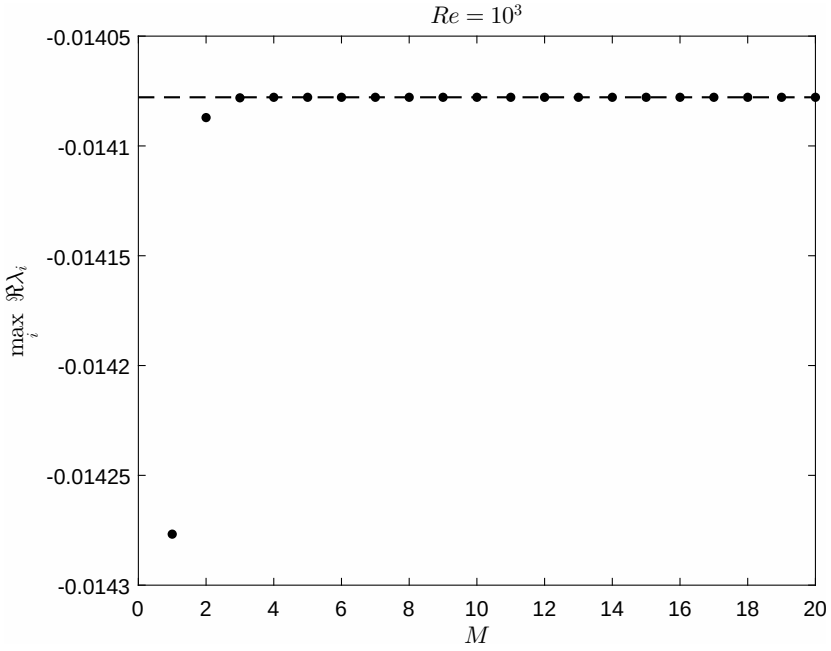

Figure 5.2: The dependence of the largest real part of the computed eigenvalues on the number of Chebyshev modes for radial approximation M for $n = k = 1$

5.2 Spectrum of the operator $\mathbb{L}$

In this section we plot the eigenvalues of the full operator $\mathbb{L}$ in the complex plane. The actual flow is equal to the superposition of all particular states for all $n \in \mathbb{Z}$ and $k = \frac{\pi}{l}m$, $m \in \mathbb{Z}$. It is impossible to cover all the possible cases of n and k, but we will focus on four the most important cases.

The first and the most simple case is $n = k = 0$ with eigenfunctions independent of θ and z (see figure 5.7 for the eigenfunction corresponding to the least stable state). The second case is $n \neq 0$ and $k = 0$ (we chose $n = 1$ for the simplicity). Figure 5.3 shows the eigenvalues in complex plane for the case $n = k = 0$ and figure 5.4 shows the eigenvalues for $k = 0$ and $n = 1$. We can see that all the eigenvalues for the both cases are real and cluster to the origin as Re increases. Table 5.1 shows the top ten eigenvalues with the largest real part. We can see

that all the eigenvalues are negative, and tend to zero as Re tends to infinity. We investigate more precisely this dependence in the following section. The reason why we introduced these two cases together is because of the similarity of the spectra unlike the other cases when $k \neq 0$.

The choice of the values M was dependent on required accuracy and time complexity. The values of M are captured in table 5.1.

The other cases are $k \neq 0$, $n = 0$ (we chose $k = 1$) and $k \neq 0$, $n \neq 0$ (we chose $n = k = 1$). The eigenvalues are plotted in figure 5.4 and 5.5. For the eigenvalues with the largest real part and the values M see table 5.2 and table 5.3. We can immediatelly see that these spectra differ from the previous cases ($k = 0$). We see that the eigenvalues are imaginary and distributed into three branches. The first branch is composed of the eigenvalues with the imaginary part $\mathrm{Im}\,\lambda \approx \frac{2}{3}$. This distinct line does not appear for the values of the Reynolds number grater than $Re \approx 10^5$. This is caused by rounding errors discussed in [10]. This has something to do with the fact that the operator $\mathbb{L}$ is non-normal and with increasing Re the operator $\mathbb{L}$ becomes *more non-normal*, again see [4]. Figure 5.8 shows the eigenfunction corresponding to the eigenvalue from the first branch. The second branch is consisted of the eigenvalues with the imaginary part $\mathrm{Im}\,\lambda > \frac{2}{3}$ called center modes. The third branch is consisted of the eigenvalues with the imaginary part $\mathrm{Im}\,\lambda < \frac{2}{3}$ called wall modes. Figures 5.9 shows the eigenfunction corresponding to the wall mode and figure 5.10 shows the eigenfunction corresponding to the center mode. Later, we will show the asymptotic behavior of these two branches.

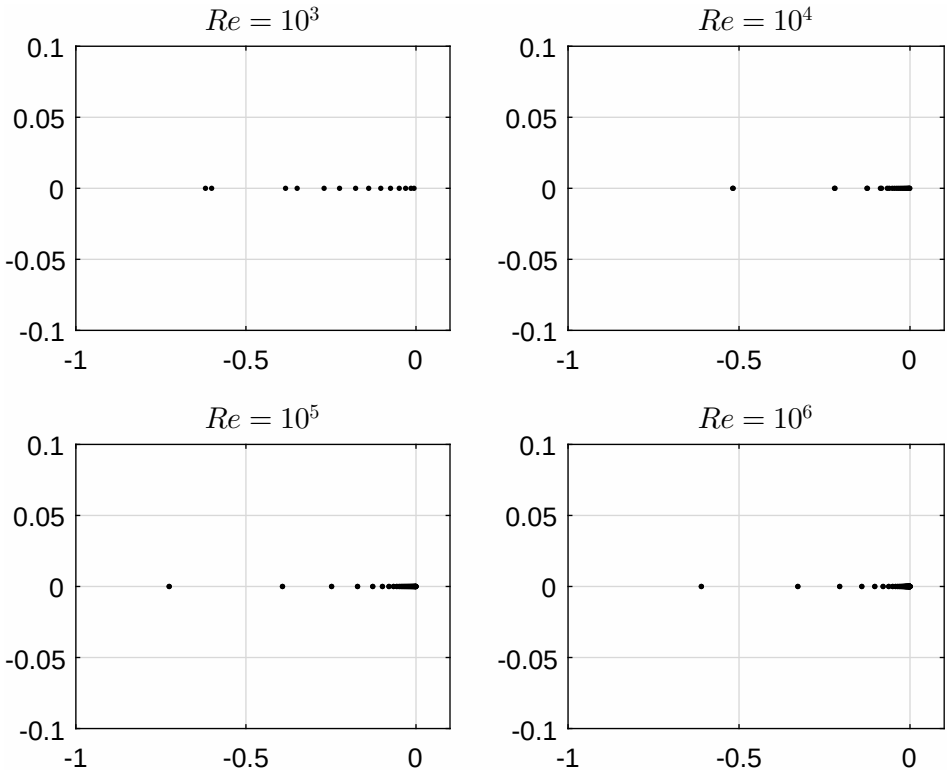

Figure 5.3: The eigenvalues of the full operator for the different Reynolds numbers in the complex plane for $k = n = 0$

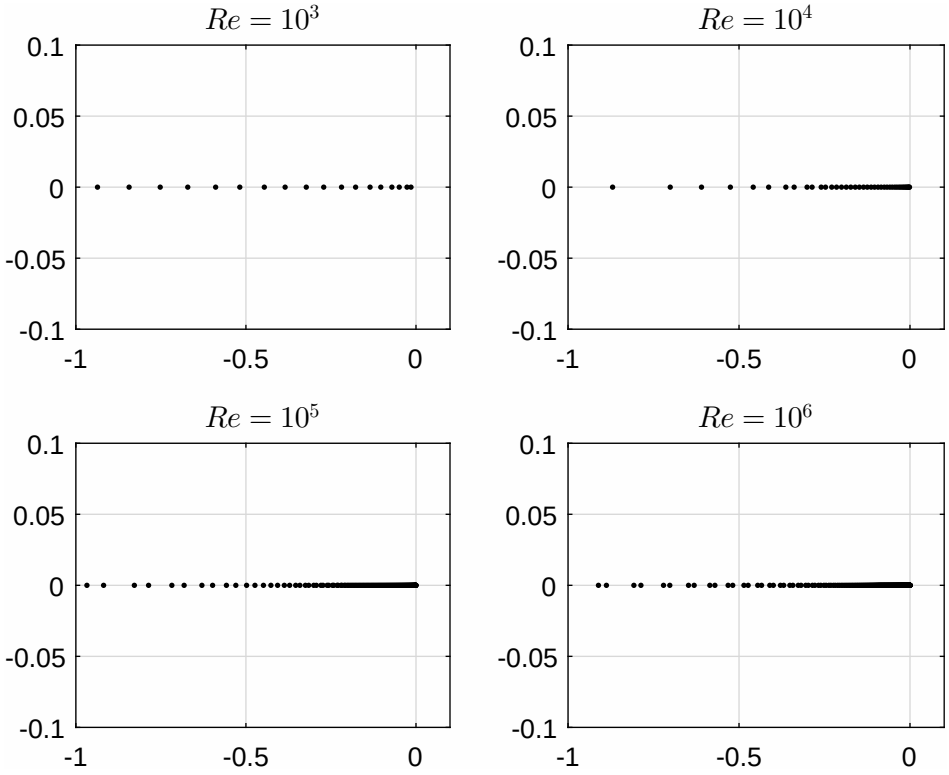

Figure 5.4: The eigenvalues of the full operator for the different Reynolds numbers in the complex plane for $k = 0, n = 1$

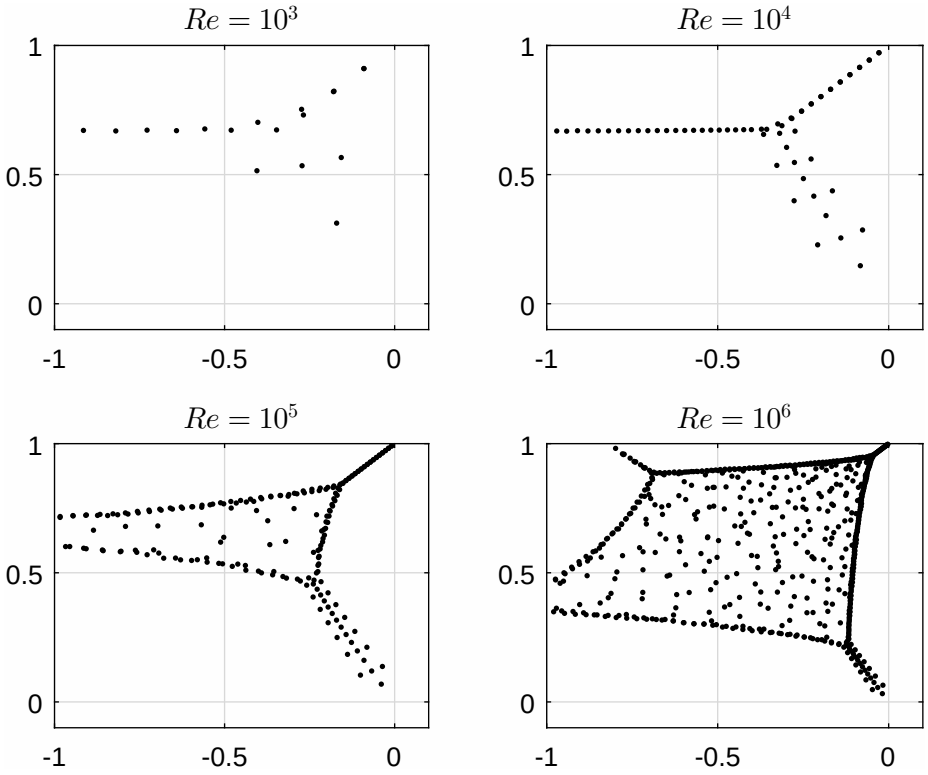

Figure 5.5: The eigenvalues of the full operator for the different Reynolds numbers in the complex plane for $k = 1, n = 0$

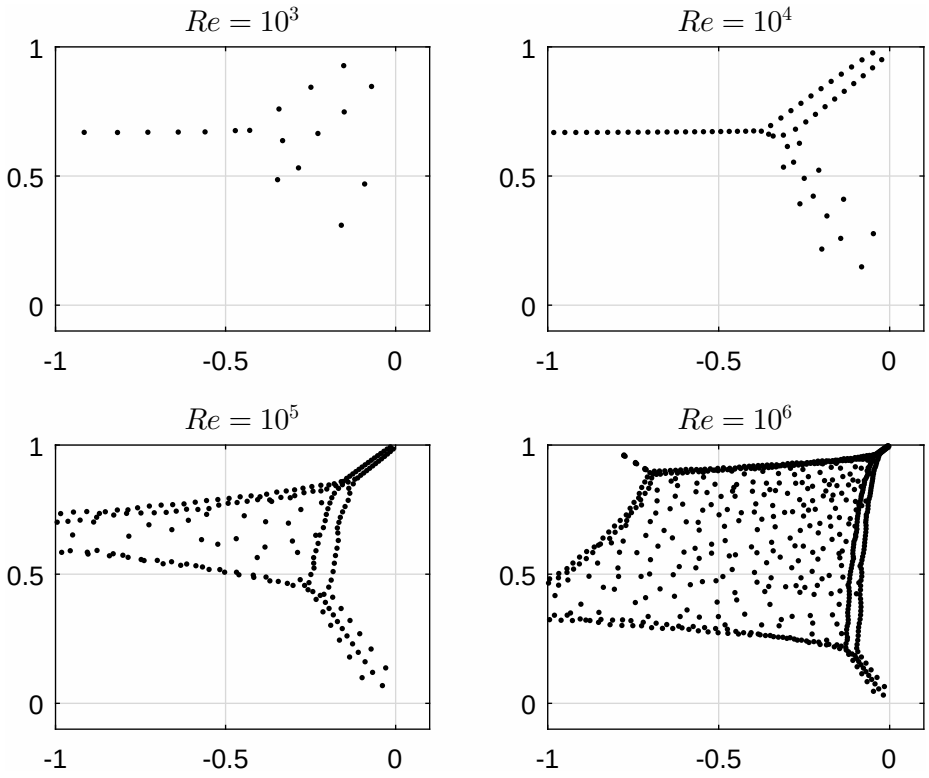

Figure 5.6: The eigenvalues of the full operator for the different Reynolds numbers in the complex plane for $k = 1, n = 1$

Table 5.1: Top ten eigenvalues with the largest real part for $n = k = 0$ and $n = 1$,$k = 0$

$n = k = 0$		$n = 1$ $k = 0$	
$Re = 10^3$, $M = 8$	$Re = 10^4$, $M = 12$	$Re = 10^3$, $M = 16$	$Re = 10^4$, $M = 24$
-0.005783185962	-0.000578318596	-0.014681970641	-0.001468197062
-0.014681970642	-0.001468197064	-0.026374616427	-0.002637461646
-0.030471262365	-0.003047126234	-0.049218456321	-0.004921845633
-0.049218456295	-0.004921845632	-0.070849998918	-0.007084999888
-0.074887164922	-0.007488700679	-0.103499453895	-0.010349945389
-0.103499394379	-0.010349945389	-0.135020708865	-0.013502070888
-0.139083201912	-0.013904028548	-0.177520766813	-0.017752076681
-0.177498009363	-0.017752076645	-0.218920189145	-0.021892018913
-0.224754465252	-0.02229327511	-0.271281654271	-0.027128165427
-0.27017818828	-0.027128154656	-0.322555116494	-0.032255511629
$Re = 10^5$, $M = 32$	$Re = 10^6$, $M = 56$	$Re = 10^5$, $M = 72$	$Re = 10^6$, $M = 150$
-0.000057831859	-0.000005783185	-0.000146819735	-0.000014680122
-0.000146819706	-0.00001468197	-0.000263746111	-0.000026378135
-0.000304712623	-0.000030471262	-0.000492184631	-0.000049219897
-0.000492184563	-0.000049218456	-0.000708499975	-0.000070849401
-0.000748870067	-0.000074887006	-0.001034994575	-0.000103502944
-0.001034994538	-0.000103499453	-0.001350207046	-0.000135020605
-0.001390402844	-0.000139040284	-0.001775207686	-0.000177523205
-0.001775207668	-0.000177520766	-0.002189201822	-0.000218916484
-0.002229323036	-0.000222932303	-0.002712816532	-0.000271284526
-0.002712816542	-0.000271281654	-0.00322555117	-0.000322555032

Table 5.2: Top ten eigenvalues with the largest real part for $n = 0$,$k = 1$

$Re = 10^3$	$Re = 10^4$
-0.090351143193+0.910548673481i	-0,028384271247+0,971715728752i
-0.090442729651+0.910557301936i	-0,028384271247+0,971715728753i
-0.156993470436+0.566149199447i	-0,056668542494+0,943431457504i
-0.170550892709+0.312166195963i	-0,056668542494+0,943431457505i
-0.178325404281+0.823014217031i	-0,076392803906+0,285639570495i
-0.179893858414+0.821108593968i	-0,082793747357+0,147212121922i
-0.268204164433+0.730844436575i	-0,084952813742+0,915147186257i
-0.272228727747+0.534314004291i	-0,084952813753+0,915147186266i
-0.273590095844+0.752807990632i	-0,113237084989+0,88686291501i
-0.347172111587+0.673018741169i	-0,113237085417+0,886862914928i
$Re = 10^5$	$Re = 10^6$
-0.008954271911+0.99105572809i	-0,002829427107+0,997171572877i
-0.008954271911+0.99105572809i	-0,002829427124+0,997171572875i
-0.017898543818+0.982111456179i	-0,00565785425+0,99434314575i
-0.017898543821+0.982111456179i	-0,005657854265+0,994343145713i
-0.026842815736+0.973167184272i	-0,008486281375+0,991514718624i
-0.026842815831+0.973167184174i	-0,008486281377+0,991514718664i
-0.035787087619+0.964222912447i	-0,011314708499+0,988686291503i
-0.035787087635+0.964222912354i	-0,011314708537+0,988686291416i
-0.035973491574+0.13725788376i	-0,01414313561+0,985857864578i
-0.039250995313+0.068822900321i	-0,014143135622+0,985857864377i

Table 5.3: Top ten eigenvalues with the smallest real part for $n = k = 1$

$Re = 10^3$	$Re = 10^4$
-0.070864011362+0.846749815969i	-0.022704914734+0.951481194804i
-0.091142609393+0.469142875603i	-0.047232199591+0.273788709335i
-0.15121626726+0.748193843797i	-0.048460432865+0.977153782622i
-0.152699583102+0.927301309131i	-0.048936177292+0.920498125432i
-0.159722386628+0.309479873799i	-0.07574809593+0.890436385477i
-0.228549842337+0.664769574468i	-0.079250801338+0.950783570186i
-0.249116943978+0.843693445559i	-0.08101850259+0.146420340749i
-0.285612826229+0.531526601564i	-0.102857540824+0.860812935555i
-0.332370319165+0.637076546507i	-0.109105063244+0.923824990361i
-0.343045568941+0.759483486014i	-0.130149260137+0.831438670495i
$Re = 10^5$	$Re = 10^6$
-0.007202317053+0.984649809606i	-0.002278591043+0.995144310844i
-0.015344184305+0.992784662196i	-0.004854884788+0.997720023898i
-0.015533241711+0.974862681073i	-0.004917688634+0.99204996396i
-0.024048978685+0.965371102891i	-0.007614426857+0.989051541005i
-0.02511278407+0.984442246447i	-0.00794637132+0.995080951604i
-0.029236459973+0.137214308074i	-0.010337409542+0.986096038617i
-0.032660506748+0.95602243791i	-0.010944925383+0.992383008821i
-0.034585362608+0.975915500696i	-0.013080970719+0.983158342393i
-0.038910627105+0.0686461437i	-0.013899329233+0.989656240713i
-0.041331029442+0.946757561753i	-0.0153380023+0.06496314961i

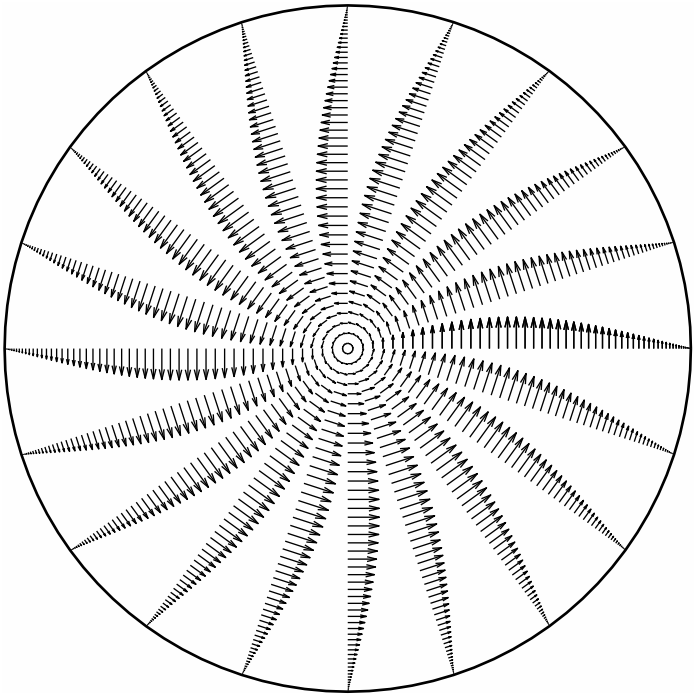

Figure 5.7: Constant-z cross section of eigenfunction corresponding to $\lambda = -0.004893990214042$ for $n = k = 0$, $M = 50$

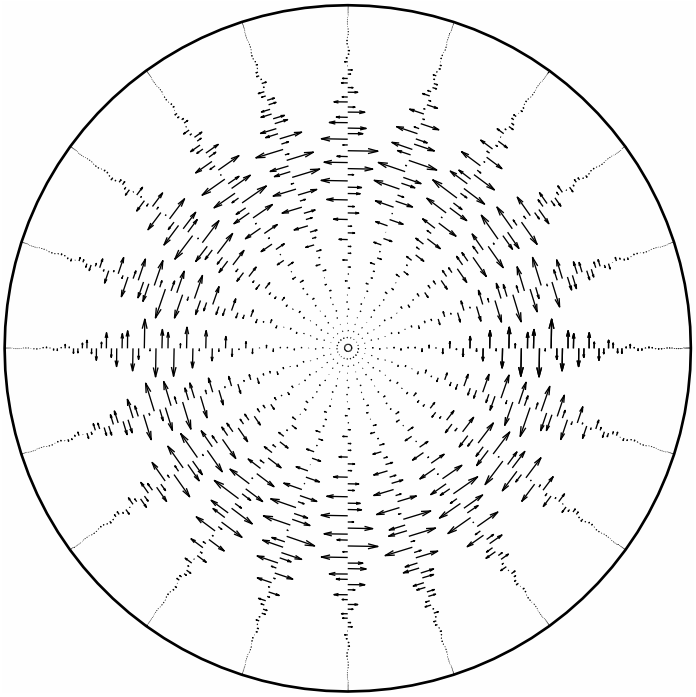

Figure 5.8: Constant-z cross section of eigenfunction corresponding to $\lambda = -1.173535911897143 + 0.668135294640209i$ for $n = k = 1$, $M = 50$

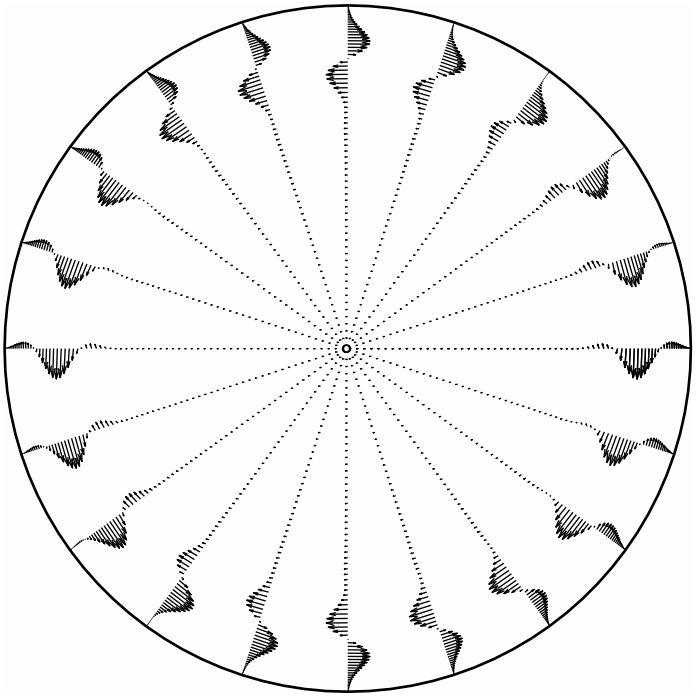

Figure 5.9: Constant-z cross section of eigenfunction corresponding to $\lambda = -0.047232199583599 + 0.273788709325560i$ (wall mode) for $n = k = 1$, $M = 50$

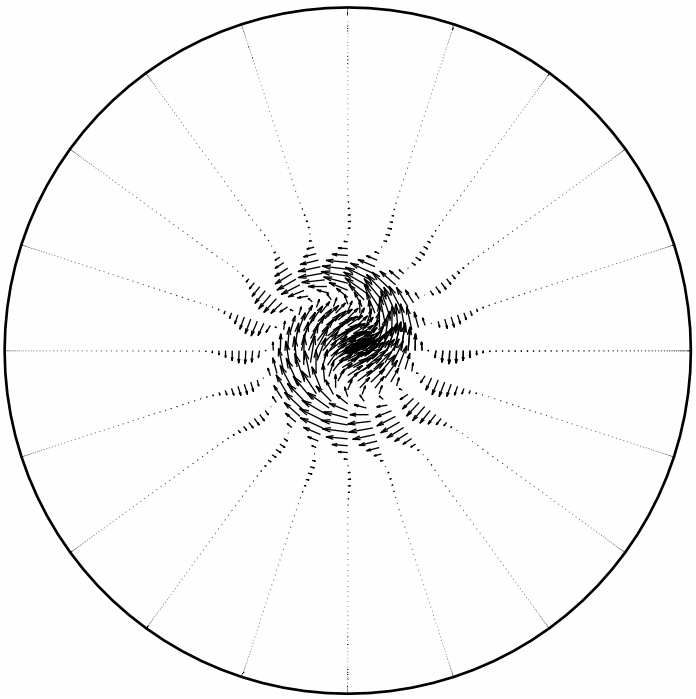

Figure 5.10: Constant-z cross section of eigenfunction corresponding to $\lambda = -0.022704914397274 + 0.951481194585837i$ (center mode) for $n = k = 1$, $M = 50$

5.3 Asymptotic behavior and comparison with the Stokes operator

The crucial question is whether the real part of the eigenvalues of $\mathbb{L}$ remains negative or not. We carried out the computation for $M = 140$ and $Re \in [10^1, 10^8]$ for the cases $n = k = 0$ and $n = 1$, $k = 0$, and for $Re \in [10^1, 10^6]$ for the cases $n = 0$, $k = 1$ and $n = k = 1$. Figures 5.11-14 show the dependence of the largest real part on the Reynolds number Re. Table 5.4 shows the numerical values. We can see that with increasing Re the largest real part also increases, but remains negative.

Figures 5.11 - 5.14 show the comparison of the largest real part of the eigenvalues for the Stokes operator and for the full operator. In table 5.4 we can see that if $k = 0$ then the largest real parts of the eigenvalues of the Stokes and full operator are very similar. This is caused by the similarity of the Stokes operator and $\mathbb{L}$ for $n = k = 0$.

The asymptotic behavior of the largest real parts of the eigenvalues of the Stokes operator is

$$\max_i \Re\lambda_i^{Stokes} \sim Re^{-1}. \tag{5.1}$$

see (3.43).

Asymptotic behavior of the eigenvalues has been analyzed theoretically for channel flow, for example in [1]. The asymptotic behavior of the eigenvalues with the largest real part of the operator $\mathbb{L}$ was *numerically* studied in [4]. Again, we have to distinguish the different cases of n and k. For the case $n = 1$, $k = 0$ the asymptotic behavior is

$$\max_i \Re\lambda_i \approx -14.6819706 Re^{-1}. \tag{5.2}$$

We can see that the asymptotic behavior of (5.1) and (5.2) is the same.

The different situation occurs when $k \neq 0$. In case $n = k = 1$ the asymptotic behavior of the center mode and wall mode are different. The approximation for the particular cases are

$$\max_i \Re\lambda_i^{center} \approx -2.28058 Re^{-1/2} + 0.92 Re^{-1}, \tag{5.3}$$

and

$$\max_i \Re\lambda_i^{wall} \approx -1.680 Re^{-1/3} + 14.3 R^{-2/3}. \tag{5.4}$$

for more information see [4].

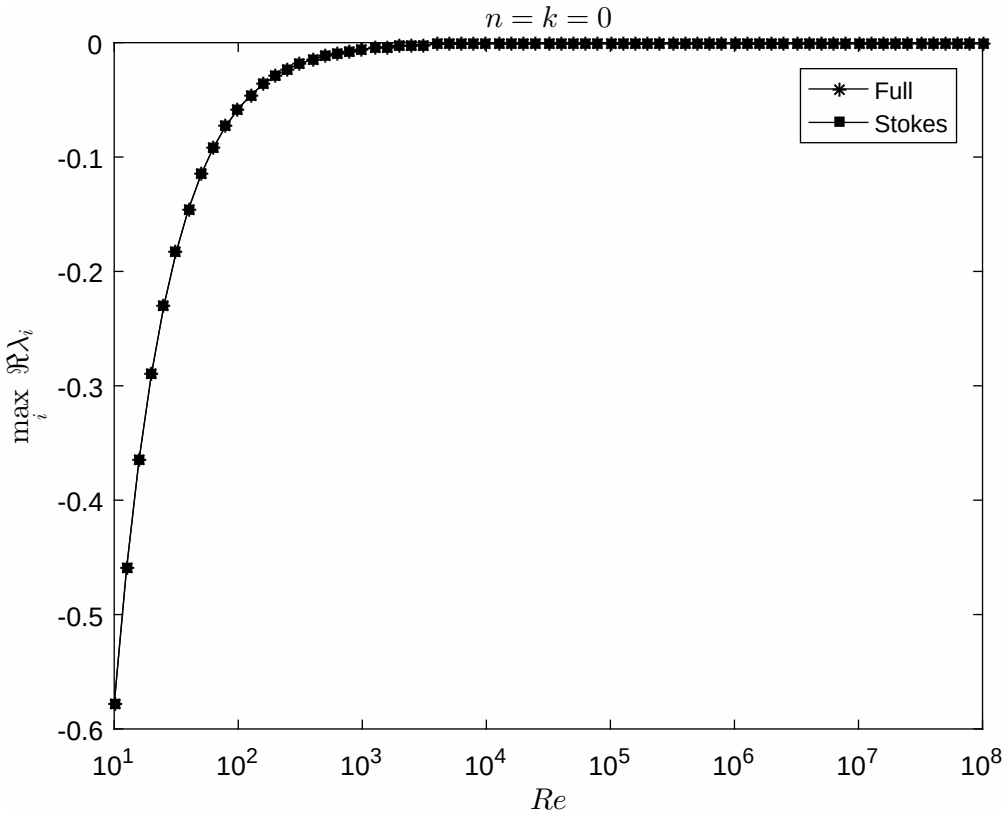

Figure 5.11: The eigenvalues of the full operator for different Reynolds numbers in the complex plane

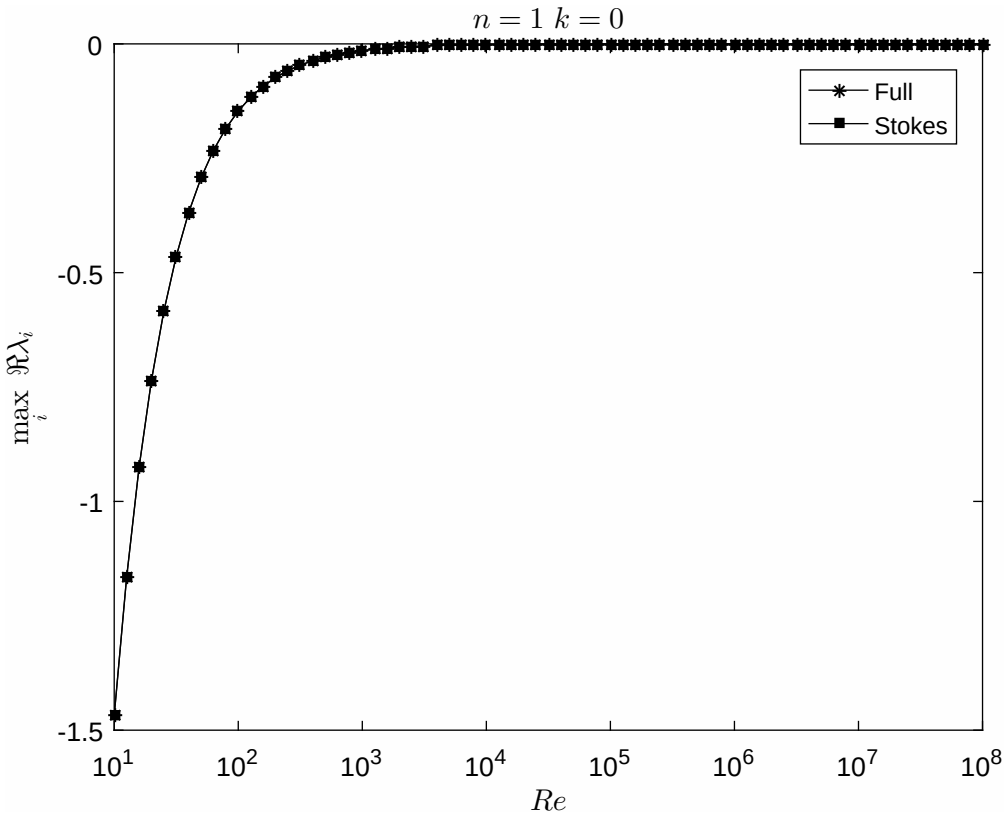

Figure 5.12: The eigenvalues of the full operator for different Reynolds numbers in the complex plane

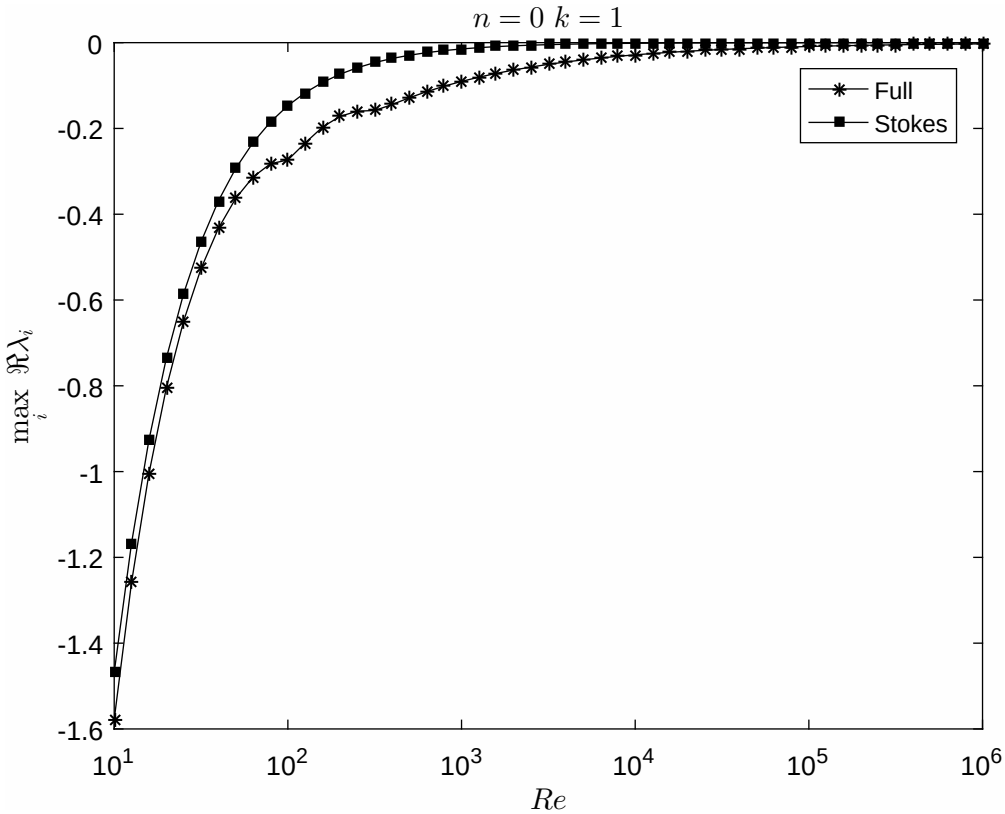

Figure 5.13: The eigenvalues of the full operator for different Reynolds numbers in the complex plane

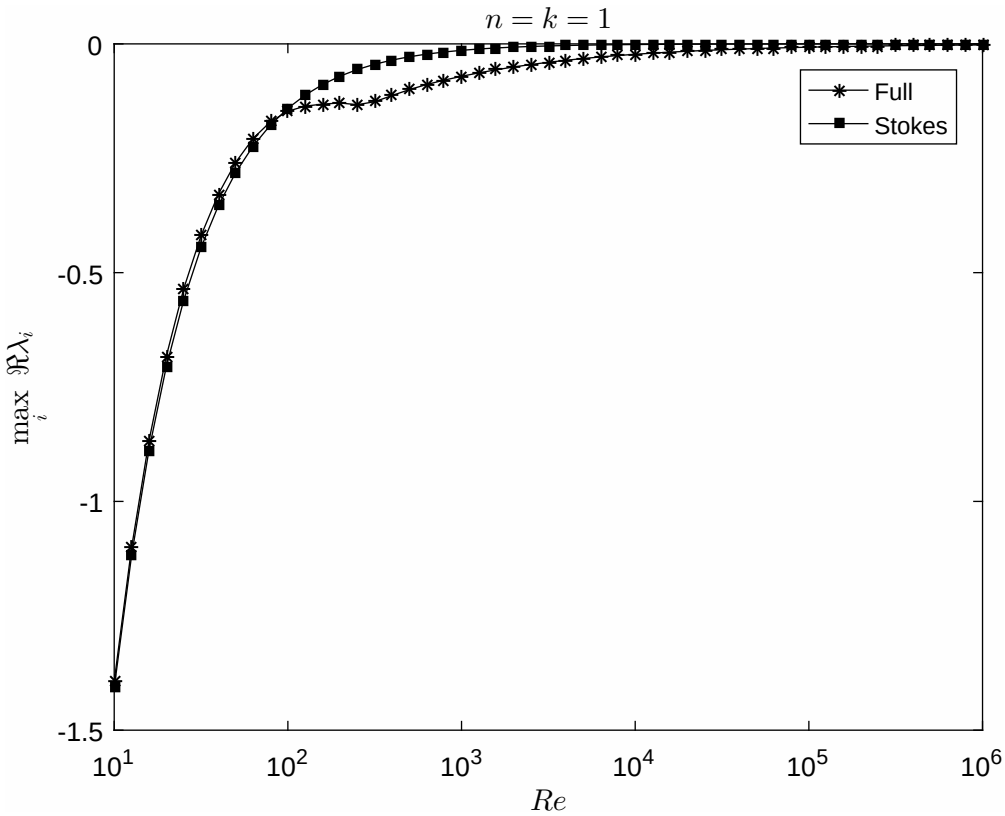

Figure 5.14: The eigenvalues of the full operator for different Reynolds numbers in the complex plane

Table 5.4: Comparison of the eigenvalues with the greatest real part of Stokes and full system

Re	Stokes	Full	Stokes	Full
	$n = k = 0$		$n = 1$ $k = 0$	
10^1	-0.578318596294	-0.578318596295	-1.468197064212	-1.468197071222
10^2	-0.057831859629	-0.057831859629	-0.146819706421	-0.146819750661
10^3	-0.005783185962	-0.005783185962	-0.014681970642	-0.014681944144
10^4	-0.000578318596	-0.000578318596	-0.001468197064	-0.00146818965
10^5	-0.000057831859	-0.000057831859	-0.000146819706	-0.000146829053
10^6	-0.000005783185	-0.000005783185	-0.00001468197	-0.000014685957
10^7	-0.000000578318	-0.000000578318	-0.000001468197	-0.00000146847
10^8	-0.000000057831	-0.000000057831	-0.000000146819	-0.0000001397
	$n = 0$ $k = 1$		$n = k = 1$	
10^1	-1.468197064212	-1.577816484154	-1.407785105145	-1.393490894002
10^2	-0.146819706421	-0.273450141036	-0.140778510514	-0.147136655284
10^3	-0.014681970642	-0.090351143264	-0.014077851051	-0.070864013135
10^4	-0.001468197064	-0.028384271062	-0.001407785105	-0.022704909271
10^5	-0.000146819706	-0.008954271911	-0.00014077851	-0.0072023138
10^6	-0.00001468197	-0.002829427126	-0.000014077851	-0.002279649415

6. Appendix

6.1 Matlab code

For more information see: [4].

```
function [r,A,B] = pipe(Re,n,k,M)
% SPECTRAL CODE FOR ANALYSIS OF LINEARIZED IDEAL PIPE FLOW
%
% A. Meseguer and L. N. Trefethen, Oxford University, 2001.
% See "Linearized pipe flow to Reynolds number 10^7"
% and http://web.comlab.ox.ac.uk/oucl/work/nick.trefethen.
%
% Inputs:
% Re = Reynolds number
% n = azimuthal wavenumber (integer)
% k = axial wavenumber (real)
% M = number of Chebyshev modes for radial approximation
%
% Outputs:
% r = Chebyshev grid in radial direction
% A, B = matrices defining eigenvalue problem
%
% Internal variables:
% rr = quadrature points in [-1,1] for quadrature
% r = restriction of rr to (0,1)
% D = Chebyshev differentiation matrix
% DE,DO = even and odd halves of D, or reverse if n is odd
% D2E,D2O = likewise for D^2
% Initializations:
global DE DO
N = 2*M+7; % number of grid points in (-1,1]
K = (N-1)/2; % number of grid points in (0,1)
half = 2:K+1; % indices of grid points in (0,1)
rad = 1:K; % indices of radial components of V & W
az = K + rad; % indices of azimuthal components
ax = K + az; % indices of axial components
% Chebyshev mesh and differentiation matrix for rr in [-1,1]
% (see cheb.m in chap. 6 of Trefethen, Spectral Methods in ...
    Matlab):
rr = cos(pi*(0:N)/N)';
c = [2; ones(N-1,1); 2].*(-1).^(0:N)';
X = repmat(rr,1,N+1);
dX = X-X';
D = (c*(1./c)')./(dX+(eye(N+1))); % off-diagonal entries
D = D - diag(sum(D')); % diagonal entries
% Extraction from D and D^2 of pieces corresponding to r in (0,1)
% (see chap. 11 of Trefethen, Spectral Methods in Matlab):
r = rr(half);
s = (-1)^mod(n,2);
DE = D(half,half) + s*D(half,N+2-half);
DO = D(half,half) - s*D(half,N+2-half);
D2 = D(half,:)*D;
D2E = D2(:,half) + s*D2(:,N+2-half);
D2O = D2(:,half) - s*D2(:,N+2-half);
```

```
% Computation of solenoidal basis and dual basis:
V = zeros(3*K,2*M+2); W = zeros(2*M+2,3*K);
for m = 0:M
p = [m+1 m+M+2];
V(:,p) = basis(n,k,r,m);
W(p,:) = dualbasis(n,k,r,m);
end
% Linearized Navier-Stokes operator:
I = speye(K); % 1
R = spdiags(r,0,K,K); % r
Ri = spdiags(1./r,0,K,K); % r^(-1)
Ri2 = spdiags(1./r.^2,0,K,K); % r^(-2)
Lam = (I-R.^2); dLam = -2*R; % laminar profile and its gradient
LV = zeros(3*K,2*M+2);
TMP = -n^2*Ri2 - k^2*I + i*k*Re*Lam;
LV(rad,:) = (D2O + Ri*DO - Ri2 + TMP)*V(rad,:) - ...
    2i*n*Ri2*V(az,:);
LV( az,:) = (D2O + Ri*DO - Ri2 + TMP)*V( az,:) + ...
    2i*n*Ri2*V(rad,:);
LV( ax,:) = (D2E + Ri*DE + TMP)*V( ax,:) + Re*dLam*V(rad,:);
LV = LV/Re;
B = W*V;
A = W*LV;
function V = basis(n,k,r,m)
global DE DO
zero = zeros(size(r));
an = min(abs(n),2-mod(n,2));
h = (1-r.^2).*cos(2*m*acos(r)); g = (1-r.^2).*h;
if n==0
u1=zero; u2=-i*k*r.*g;
v1=r.*h; v2=zero;
w1=zero; w2=DO*(r.*g)+g;
else
u1=-i*n*r.^(an-1).*g; u2=zero;
v1=DE*(r.^an.*g); v2=-i*k*r.^(an+1).*h;
w1=zero; w2=i*n*r.^an.*h;
end
if k==0 & n==0, w2=h; end
V = [u1 u2; v1 v2; w1 w2];
function W = dualbasis(n,k,r,m)
global DE DO
zero = zeros(size(r));
h = (1-r.^2).*cos(2*m*acos(r)); g = (1-r.^2).*h;
if n==0
u1=zero; u2=i*k*r.^2.*g;
v1=h; v2=zero;
w1=zero; w2=DE*(r.^2.*g)+r.^3.*h+r.*g;
else
s = mod(n,2);
u1=i*n*g.*r.^s; u2=zero;
v1=DO*(g.*r.^(s+1))+r.^(s+2).*h; v2=-i*k*r.^(s+2).*h;
w1=zero; w2=i*n*r.^(s+1).*h;
end
if k==0 & mod(n,2)==1, w2 = i*n*h; end
if k==0 & n==0, w2 = r.*h; end
N = 2*(length(r)+1);
W = ((pi/N)*[r r; r r; r r].*[u1 u2; v1 v2; w1 w2]).';
```

Conclusion

We have studied the problem of the stability of the laminar solution of the Hagen–Poiseuille pipe flow under infinitesimal perturbation. We have formulated the linearized evolution equations for the infinitesimal perturbation and the corresponding eigenvalue problem for the operator $\mathbb{L}$ characterizing the evolution of the perturbation.

We have introduced the Stokes operator, which is a similar but simpler operator then $\mathbb{L}$, and we have summarized the derivation of the analytic formulas for the eigenvalues and eigenfunctions of the Stokes operator.

Further we have briefly discussed the most important numerical methods used in the numerical computation of the eigenvalues of the operator $\mathbb{L}$. We have introduced the concepts of Chebyshev polynomials, differentiation matrices, numerical quadrature and Petrov-Galerkin discretization, and we have explained the application of these concepts in the algorithm.

The main objective of the thesis was to carry out numerical computations of the eigenvalues of the operator $\mathbb{L}$. Using the analytic results for the Stokes operator we have demonstrated the convergence of the numerical method.

We have verified the negativity of the computed eigenvalues for the Reynolds numbers in the range $Re \in [10^1, 10^8]$ for the case $k = 0$ and in the range $Re \in [10^1, 10^6]$ for the case $k \neq 0$. Having obtained numerically calculated spectrum $\sigma(\mathbb{L})$ for the full operator and analytic results for the spectrum $\sigma(\mathbb{A})$ of the Stokes operator, we have investigated the relation between $\max_{\lambda_i \in \sigma(\mathbb{L})} \Re(\lambda_i)$ and $\max_{\lambda_i \in \sigma(\mathbb{A})} \Re(\lambda_i)$.

Having compared the analytically derived asymptotic behavior of the dependence of the largest real part of the eigenvalues for the Stokes operator and numerically computed asymptotic behavior for the full operator (see [4]) we have found that the asymptotic behavior is the same for the case $k = 0$. For the case $k \neq 0$ the numerical results indicate that *the largest real part of the eigenvalues of the Stokes operator is greater than the the largest real part of the eigenvalues of the full operator.* Provided that we work with sufficiently large values of the Reynolds number.

This hypothesis is based only on numerical results and must be verified analytically. If it is correct it will provide us an important estimate on the behavior of the spectrum of the full operator $\mathbb{L}$, and might help to resolve the open problem on the stability of the pipe flow (see *Yudovich: Eleven great problems of mathematical hydrodynamics* [2]).

Bibliography

[1] S. A. Orszag. Accurate solution of the Orr-Sommerfeld stability equation. *J. Fluid Mech.*, 50:689–703, 1971.

[2] V. I. Yudovich. Eleven great problems of mathematical hydrodynamics. *Moscow mathematical journal*, 3:711–737, 2003.

[3] B. Rummler. The Eigenfunctions of the Stokes Operator in Special Domains. I. *ZAMM - Journal of Applied Mathematics and Mechanics*, 77:619–627, 1997.

[4] A. Meseguer, L. N. Trefethen. Linearized pipe flow to Reynolds number 10^7. *Journal of computational physics*, 187:178–197, 2003.

[5] M. Braun. *Differential Equations and Their Applications: An Introduction to Applied Mathematics*. Springer-Verlag, 1983.

[6] P. Constantin, C. Foias. *Navier-Stokes Equations*. The University of Chicago Press, 1988.

[7] D. Funaro. *Polynomial Approximation in Differential Equations*. Springer-Verlag, 1992.

[8] C. Canuto, M. Y. Hussaini, A. Quarteroni, T. A. Zang. *Spectral Methods: Fundamentals in Single Domains*. Springer-Verlag, 2006.

[9] L. N. Trefethen. *Spectral Methods in MatLab*. Society for Industrial and Applied Mathematics, Philadelphia, PA, USA, 2000.

[10] A. Meseguer, L. N. Trefethen. A spectral Petrov - Galerkin formulation for pipe flow I: Linear stability and transient growth. *Oxford University Computing Laboratory, Numerical Analysis Group*, 2000.

List of Figures

List of Tables